"Increase in HFC-134a emissions in response to the success of the Montreal Protocol."

A. Fortems-Cheiney[1,*], M. Saunois[1], I. Pison[1], F. Chevallier[1], P. Bousquet[1], C. Cressot[1], S.A. Montzka[2], P.J. Fraser[3], M.K. Vollmer[4], P.G. Simmonds[5], D. Young[5], S. O'Doherty[5], R.F. Weiss[6], F. Artuso[7], B. Barletta[8], D.R. Blake[8], S. Li[9], C. Lunder[10], B.R. Miller[2], S. Park[9,11], R. Prinn[12], T. Saito[13], L.P. Steele[3], and Y. Yokouchi[13]

[1]Laboratoire des Sciences du Climat et de l'Environnement, Institut Pierre-Simon Laplace, CEA/CNRS/UVSQ, Gif-sur-Yvette, France.

[2]Earth System Research Laboratory, National Oceanic and Atmospheric Administration, Boulder, CO, USA.

[3]CSIRO Oceans and Atmosphere Flagship, Aspendale, Victoria 3195, Australia.

[4]Laboratory for Air Pollution and Environmental Technology, Empa, Swiss Federal Laboratories for Materials Science and Technology, Dubendorf, Switzerland.

[5]School of Chemistry, University of Bristol, Bristol, UK.

[6]Scripps Institution of Oceanography, University of California, San Diego, La Jolla, California, USA.

[7]ENEA–Italian national Agency for New Technologies, Energy and Sustainable Economic Development, Rome, Italy.

[8]Department of Chemistry, University of California, Irvine, California, USA.

[9]Kyungpook Institute of Oceanography, College of Natural Sciences, Kyungpook National

University, Daegu, South Korea.

[10]Norwegian Institute for Air Research, Kjeller, Norway.

[11]Department of Oceanography, College of Ecology and Environmental Science, Kyungpook National University, Sangju, South Korea.

[12]Center for Global Change Science, Massachusetts Institute of Technology, Cambridge, MA, USA.

[13]National Institute for Environmental Studies, Tsukuba, Japan.

[*]now at Laboratoire Interuniversitaire des Systèmes Atmosphériques, CNRS/INSU UMR7583, Université Paris-Est Créteil et Université Paris Diderot, Institut Pierre Simon Laplace, Créteil, France.

Abstract.

The 1,1,1,2-tetrafluoroethane (HFC-134a), an important alternative to CFC-12 in accordance with the Montreal Protocol on Substances that Deplete the Ozone Layer, is a high Global Warming Potential (GWP) greenhouse gas. Here we evaluate variations in global and regional HFC-134a emissions and emission trends, from 1995 to 2010, at a relatively high spatial and temporal (3.75° in longitude ×2.5° in latitude and 8-day) resolution, using surface HFC-134a measurements.

Our results show a progressive increase of global HFC-134a emissions from 19 ± 2 Gg/yr in 1995 to 167 ± 5 Gg/yr in 2010, with both a slowdown in developed countries and a 20 %/yr increase in China since 2005. A seasonal cycle is also seen since 2002, which becomes enhanced over time, with larger values during the boreal summer.

1. **Introduction**

As a consequence of the Montreal Protocol and its amendments, hydrofluorocarbons (HFCs) have been introduced as replacement compounds for both chlorofluorocarbons (CFCs) and hydro-chlorofluorocarbons (HCFCs) since they do not deplete stratospheric ozone. The most abundant HFC measured in the atmosphere is HFC-134a [Carpenter and Reimann et al., 2014]. HFC-134a has a steady-state lifetime of 14 years; it is mainly removed from the atmosphere by its reaction with hydroxyl radicals (OH), and **to** a lesser extent by oxidation and photolysis in the stratosphere, [Carpenter and Reimann et al., 2014]. Its global average mixing ratio reached about 68 ppt in 2012 and has steadily increased, with a growth rate of 5 ppt/yr over the period 2011-2012 [Carpenter and Reimann et al., 2014], similar to the growth rate of 4.7 ppt/yr over the period 2005-2008 [Montzka and Reimann et al., 2011].

While posing no threat to stratospheric ozone, HFC-134a is nevertheless of concern because of its long lifetime, combined with a relatively high GWP of 1500 over the 100-yr horizon [Forster et al., 2007; Harris and Wuebbles, 2014]. Indeed the HFC-134a contribution to atmospheric radiative forcing has grown from negligible in 1995 to 12 ± 0.2 mW/m2 in recent years [Rigby et al., 2014] following the sharp emission rise over this period. Within current scenarios of continued HFC emission growth, its contribution to the radiative forcing of the climate system could be equivalent to 9–19% of carbon dioxide emissions by the year 2050 [Velders et al., 2009, Daniel and Velders, 2011]. Amendment proposals to address HFCs under the Montreal Protocol have been submitted in May 2014 [EPA, 2014]. Since low GWP products exist for replacement of HFC-134a, for use in refrigeration and air-conditioning systems, HFC-134a is a key candidate for climate mitigation and it has come into the focus of international climate policy [Molina et al., 2009]. There is a growing interest in better estimating global and regional emissions of this species.

HFC-134a has been the preferred replacement gas of CFC-12 (CCl_2F_2) in developed countries. According to the Alternative Fluorocarbons Environmental Acceptability Study (AFEAS, www.afeas.org), in 2001, over 80% of the worldwide sales of HFC-134a fall into two categories: mobile air conditioning (MAC) and commercial refrigeration (in order of importance, HFC-134a from MAC reaching 70% of the global emissions [Montzka et al., 2015]). These emission sources are the most important in Europe [Schwarz et al., 2003] and in the US [EPA, 2008]. HFC-134a is emitted from air conditioning systems to the atmosphere during use, servicing, repair, and vehicle end-of-life [Clodic et al., 2005; Kuijpers et al., 2011]. Wimberger et al. [2010] took HFC-134a samples from vehicles on dismantler lots in California and found that on average only 27% of the initial HFC-134a remained in the mobile air conditioning system before dismantlement, meaning that 73% had been released into the atmosphere.

Very large uncertainties remain in the inventory-based quantification of global and regional HFC-134a emissions [Barletta et al, 2011], due to the diversity of emission processes and consumption habits [Clodic et al., 2005; Atkinson et al., 2003; Rugh et al., 2004]. For instance, estimations of the HFC-134a emission rate from traffic (Wallington et al. [2008]) and domestic sector suffer from large uncertainties. The usage of HFC-134a for air conditioning not only varies with climate but also with region-specific equipment rate of air-conditioning systems in cars or national commitments within the United Nations Framework Convention for Climate Change (UNFCCC).

In this context, attempts have been made to deduce HFC-134a emission maps from HFC-134a atmospheric mole fraction measurements by statistical top-down methods. Stohl et al. [2009] developed their own global gridded HFC-134a emission inventory based on UNFCCC reporting,

and optimized it from atmospheric measurements using an inverse procedure and a Lagrangian transport model for years 2005 and 2006. Other studies focused on sub-continental regions: the US [Millet et al., 2009; Manning and Weiss, 2007; Hu et al., 2015], Europe [Keller et al., 2012] and East Asia [Stohl et al., 2010; Kim et al., 2010]. Some disagreements exist between these top-down estimates: Stohl et al. [2009] found that US emissions in 2006 were 53% higher than the estimate of Manning and Weiss [2007] (28 Gg and 43 Gg, respectively). Stohl et al. [2009] also significantly increased the estimate made in the EDGAR-v4.0 inventory (source: EC-JRC/PBL, http://edgar.jrc.ec.europa.eu/, 2010) for Chinese emissions in 2005. These various studies were restricted to short periods: years 2005-2006 for Stohl et al. [2009], year 2008 for Stohl et al. [2010]. Therefore they could not assess the global and regional emission growth rates since the enforcement of the Montreal Protocol in 1994 (Copenhagen Amendment).

This study aims to evaluate the evolution of HFC-134 emissions to the Montreal Protocol at the global and regional scales as seen from atmospheric measurements over the period 1995-2010.

The atmospheric inverse system includes a global chemistry transport model at a resolution of 3.75°x2.5°. This allows the assessment of HFC-134 surface fluxes at the grid resolution, at an 8-day frequency, with a simultaneous optimization of OH concentrations in four latitudinal bands. Details on the inverse system and on the methodology are given in Section 2. The inferred fluxes are analyzed in Section 3 in terms of global and regional trends as well as seasonal variability.

2. **Methodology**

Our strategy follows the one applied by Fortems-Cheiney et al. [2013] for the study of HCFC-22

emissions. In our inverse system, a state vector **x**, representing the emissions, is optimized in order that both the distance between the atmospheric observations **y** and the simulated concentrations H(**x**), and the distance between **x** and a prior knowledge on the emissions $\mathbf{x_b}$, are minimized given the respective uncertainties of **y** and $\mathbf{x_b}$. Their error covariance matrices **R** and **B** respectively represent these uncertainties. The Bayesian cost function J defined below, is minimized iteratively and provides a solution, called posterior in the following.

$$J(\mathbf{x}) = (\mathbf{x} - \mathbf{x_b})^T \mathbf{B}^{-1} (\mathbf{x} - \mathbf{x_b}) + (H(\mathbf{x}) - \mathbf{y})^T \mathbf{R}^{-1} (H(\mathbf{x}) - \mathbf{y})$$

The minimization is performed by the M1QN3 limited-memory quasi-Newton minimization algorithm [Gilbert and Lemaréchal, 1989] and exploits the adjoint operator of *H*. We reduce the norm of the gradient of J by more than 99 %.

H represents the chemistry transport model and the non-linear observation operator. The transport model is the offline version of the atmospheric general circulation model LMDz [Hourdin et al., 2006]. The main sink of HFC-134a in the troposphere is its reaction with the radical hydroxyl OH: $CH_2FCF_3 + OH^{\cdot} \rightarrow CHFCF_3 + H_2O$. The chemical scheme coupled to LMDz represents only the interaction between the radical hydroxyl OH and HFC-134a, and the other sinks are neglected. We use the reaction rate $k=1.05\times 10^{12} \exp(1630/T)$ $cm^3.molecule^{-1}.s^{-1}$, as recommended by Sander et al., [2011]. The OH distribution is also optimized by the inverse system. The prior OH 3D fields result from a simulation with full chemistry of the model LMDz-INCA (INtéractions Chimie et Aérosols, [Hauglustaine et al., 2004]).

As a result, our state vector **x** includes:

- HFC-134a initial concentrations for 1 January 1995 at 00:00 at the model resolution (3.75° ×2.5°

in longitude, latitude)

- HFC-134a surface emissions at an 8-day and at 3.75° ×2.5° resolution, for the 1995-2010 period - Four factors to scale the OH prior atmospheric concentrations at an 8-day resolution, for four latitude bands (90°S-30°S, 30°S-0°, 0°-30°N, 30°N-90°N).

2.1 **Prior set-up**

Our gridded HFC-134a prior emissions in $\mathbf{x_b}$ are mostly taken from the EDGAR-v4.2 inventory (source: EC-JRC/PBL, http://edgar.jrc.ec.europa.eu/, 2011), which provides yearly estimates until 2008. We adapted this prior source specifically for China following Stohl et al. [2010]. Indeed, the small HFC-134a emissions in China (ranging from 0 in 1995 to about 1 Gg in 2008) suggested by the EDGAR-v4.2 inventory is not consistent with i) the large development of air-conditioning systems in Chinese vehicles and 2) the ban of CFC-12 production in this country since the end of year 2010.

Hu et al. [2010], using an inventory-based approach, estimated that the Chinese HFC-134a emissions from automobile (including cars, bus and trucks) air conditioners have increased from 7.3 Gg/yr in 2005 to 21.2 Gg/yr in 2010. Applying a growth rate of 23 %/yr of mobile air conditioners from 1995 to 2010, and assuming that automobile air conditioners account for two thirds of total HFC-134a emissions like Stohl et al. [2010], we obtain prior Chinese HFC-134a emissions ranging from less than 1 Gg/yr in 1995 to 21 Gg/yr in 2010 (see Table 1).

For the rest of the world, we made no effort to adjust the EDGAR-v4.2 inventory to the years 2009

and 2010 in the prior. Figure 1 (top) displays the grid-point prior emissions in 1995 and 2010. Whereas HFC-134a emissions are mostly localized around industrial sites in Europe (Benelux), in the USA (Silicon Valley, California; Silicon Prairie, Texas; Research Triangle, North Carolina and Route 128, Massachusetts) and in Japan in 1995, large emissions are less localized but more spatially distributed over these continents in 2010. A broader distribution of HFC-134a emissions is also supported by the inversion analysis of atmospheric data provided in Hu et al., [2015].

The grid-point standard deviations of the prior errors assigned to the HFC-134a prior emissions are set at 100% of the flux. Prior error correlations in space are represented by an e-folding length of 500 km over land and temporal correlation by an e-folding length of 8 weeks. These prior error statistics lead to annual global HFC-134a budgets of 20 ± 4 Gg/yr for year 1995 and of 183 ± 34 Gg/yr for year 2010 (from now on, the ± signs represent the one sigma standard deviation), leading to a large 20 % 1-sigma uncertainty. The resulting prior error uncertainty is ± 30 % for Europe and about ± 35% for the US and China, which fairly represents the large and uncertain inter-annual variability of the regional HFC-134a emissions in recent years.

The errors assigned to the scaling factors of OH are of 10% (1-sigma), based on the differences between various estimates of OH concentrations [Prinn et al., 2001; Krol and Lelieveld, 2003; Bousquet et al., 2005].

2.2 Assimilated Observations

Our observation dataset includes measurements of HFC-134a dry air mole fractions made at 21 sites, listed in Table 2, from December 1994 to March 2011. It was downloaded from the World Data

Centre for Greenhouse Gases (http://ds.data.jma.go.jp/gmd/wdcgg/, accessed 15 November 2012), except for the Gosan data. We use both flasks (from the NOAA/ESRL [Montzka et al., 1996; Montzka et al., 2015] and from the ENEA [Artuso et al., 2010] networks) and continuous measurements (from the AGAGE [Prinn et al., 2000; O'Doherty et al., 2004] and from the NIES networks [Yokouchi et al., 2006]), respectively named "event" and "daily" data in the database. Continuous measurements by the AGAGE and NIES networks were averaged over daytime, and these daily means were used as constraints together with the flask measurements. The total number of observational constraints for the entire period is 17803.

The different stations are sparsely distributed over the globe, but mainly located in the northern hemisphere (Figure 2). Before 1998, there were mainly flask measurements available, leading to a small number of HFC-134a observational constraints (129 in 1997). After 1998, some continuous measurements were made gradually available, so that 643 constraints were used in 2003 and 2,246 in 2007. The evolution of the total number of observational constraints used in the inversion per year is shown in Figure 3 for the regions USA, Europe and China, where most of the stations are located. Note that measurements of HFC-134a over the continental US beginning in 2008 recently became available [Hu et al., 2015] but are not included in this analysis.

The estimate of all the errors involved in the observation errors in the inversion system, defined as in Fortems-Cheiney et al. [2013], is approximately 3% (mean value of 1.3×10^{-6} ppm). It combines representation errors (e.g., the mismatch between the observation and model resolutions), errors of the observation operator (including transport and chemical-scheme errors in LMDZ-SACS), measurements errors (including instrumental precision for HFC-134a measurements and the errors involved in the calibration scales), and errors of the CTM. The measurements coming from

AGAGE, NOAA, and NIES networks are respectively calibrated using SIO-2005, NOAA/CMDL and NIES-2008 scales. It should be noted that differences between networks (calibrations uncertainties, inter-calibration factors) are small [Stohl et al., 2010; Carpenter and Reinman, 2014], compared to other causes of uncertainties such as representation or model errors. Error correlations between the measurements are neglected; so that the covariance matrix R of the observation errors is diagonal (i.e. only variances are taken into account). It should be noted that the degree of freedom of the inverse problem is about 255.

2.3 Calculation of the analysis error

The calculation of the analysis error is challenging in the framework of variational inverse system. Even though the analysis error covariance matrix can be written in various analytical forms, it requires the inversion of matrices that are too large to invert given the current computational resources in our variational approach. As a result, one way to compute the analysis error is to perform a randomization approach (Monte Carlo) to estimates the posterior errors on the fluxes. The result of this method is in agreement with the Bayesian covariance matrix A. This approach has been described in Chevallier et al., [2007] and contains the following steps:

– running the LMDZ-SACS chemistry-transport model with a climatology of surface emissions to generate a set of pseudo HFC-134a observations at the same location and time as the actual measurements,

– perturbing the pseudo-observations consistently with assumed observation error statistics (described later in the section),

– perturbing the state vector (that includes the surface flux climatology) consistently with assumed error statistics,

– performing a Bayesian inversion of the surface fluxes using the perturbed pseudo-observations as constraints and perturbed state vector as the prior field,

– comparing the estimate of the inversion to the flux climatology to get the Bayesian errors of the estimate.

The method is applied ten times with different perturbations each time, in order to compute the posterior error statistics. We estimate the posterior one-sigma uncertainty from these Monte Carlo inversion ensembles (10 members) for three different years: 1995, 2005 and 2010. Following the usual practice, we define the uncertainty reduction as $(1-\sigma_a/\sigma_b)\times 100$, with σb the prior error standard deviation and σa the theoretical posterior error standard deviation.

Results

3.1. Theoretical performance of the inversion

The uncertainty on the posterior emissions, calculated with the Monte-Carlo approach, is presented in Table 1 for the years 1995, 2005 and 2010. The uncertainty reductions reached by the inversion for the years 1995, 2005 and 2010 are synthesized in Table 3 for regional and global aggregations. The uncertainty reduction at the grid scale resolution is also shown in Figure 1d) and 1h), respectively for years 1995 and 2010. In 1995, the global uncertainty reduction reaches 56%. At the regional scale, the uncertainty associated with the emissions is reduced by 54% for the US and 11% for Japan. However, the uncertainty reduction remains small for Europe and China, owing to the lack of sampling locations near these regions (Table 2).

The expansion of the surface network increases the number observational constraints in the inversion over time. Combined with the increased emissions in the atmosphere, this leads to larger uncertainty reductions, as shown in Figure 1 and in Table 3, both at the global (71% and 84% in 2005 and in 2010) and at regional scales. Indeed, in 2005, the uncertainty reduction is 56% for the US, and 45% for Europe. For Japan and China, the uncertainty reduction is 40% and 23%; this increase of uncertainty reduction coincides with the set-up of the first Asian site, Hateruma, in May 2004. Thanks to the benefits of the sites Gosan in South Korea (since November 2007) and Cape Ochi-ishi in Japan (since August 2008), the uncertainty reduction reaches 81% and 46%, respectively, in 2010.

3.2. Global HFC-134a emissions.

Table 1 presents the annual global prior and posterior HFC-134a emissions. Figure 1b) and 1f) shows the relative difference between posterior and prior HFC-134a emissions at the grid point resolution, respectively in 1995 and in 2010. Figure 4 and Figure 6 show the global posterior HFC-134a emissions. Posterior emissions range from 18 ± 2 Gg/yr in 1995, to f167 ± 5 Gg/yr in 2010 (see Table 1 and Figure 4). These estimates are in excellent agreement with the posterior emissions of Xiang et al., [2014], ranging from 20 Gg in 1995 to 153 Gg in 2010 who used the same NOAA and AGAGE networks and additional observational data (i.e, the aircraft campaigns Hiaper-Pole-to-Pole of Carbon Cycle and Greenhouse Gases Study HIPPO over the Pacific Ocean) to derive global emissions for these years. As seen in Table 1, this is also consistent with the posterior emissions of Montzka et al., [2015] and Rigby et al., [2014], ranging respectively from 22 Gg in 1995 to 168 and 167 Gg in 2010.

It is interesting to see that the yearly increase we derive is more pronounced from 2009 to 2010 (growth rate of +14%) than from 2005 to 2009 (mean growth rate of 3.5%). The absolute global emission magnitudes and increase in emissions are also consistent with the +17% inferred by Lunt et al., [2015] between their average estimate of 141.6 Gg/yr for the 2007-2009 period and of 166.5 Gg/yr for the 2010-2012 period (derived with ten measurement stations from AGAGE and NIES networks).

One should note that discrepancies between different global-based inverted results can be due to the observational measurements used to constrain the emissions, but also to the diversity of the inversion systems (such as the CTM used, whether or not the OH fields are prescribed in the model, etc). Nevertheless, all these independent studies show a continuous rise of HFC-134a emissions between 1995 and 2010.

Until the year 2000, posterior estimates are smaller than the prior ones with relative differences of about -4%. The differences between the prior and the posterior estimates increase after 2000 (i.e, -13% in 2005), demonstrating an overestimation of the EDGAR-v4.2 HFC-134a emissions on global scale.

3.3. Regional HFC-134a emissions and Growth Rates

Almost all the posterior regional estimates are smaller than the prior ones: -7% for the US, especially over the east coast (modification in a range of -10% to -20%); - 8% for Europe; -23% for Japan in 2010. On the contrary, the Chinese posterior estimate is about the same as the prior one. In the following, regional HFC-134a emissions are discussed in details for the US, Europe, China and

Japan.

3.3.a The United States of America emissions

The posterior inventory highlights the US as the main HFC-134a source, contributing at least 45% of the global emissions since 1995.

Our posterior US emissions are higher than most of the previous studies for the years 2005-2007 (see Table 4). In 2005, we infer emissions 62% higher (57±9 Gg/yr, starting from a prior of 68 ±24 Gg/yr) than the 35 Gg/yr of Stohl et al. [2009] (starting from a prior of 57 Gg/yr). Our posterior US estimates are also more than two times larger than the HFC-134a emissions estimated from aircraft measurement campaigns in 2004 and 2006 by Millet et al. [2009], and higher than the estimates of 43 Gg/yr (22-60) of Manning and Weiss [2007] for year 2006 and of 43±6 Gg/yr of Barletta et al. [2011] for 2008. The more comprehensive suite of data used here compared to these studies (e.g, measurements only from the THD stations for Manning and Weiss [2007]) may explain such differences. On the contrary, our 2008-2010 average of 63±9 GG is in good agreement with the 52-61 Gg average estimated by Hu et al. [2015] for 2008-2010, derived from multiple inversion scenarios and using data from more sites (with daily flasks air-samples and aircraft campaigns) over the US than in our study.

As shown in Figure 4 and in Figure 7, our estimate for the US shows a progressive increase between 1995 and 2010, ranging from 10 ± 2 Gg/yr (starting from a prior of 10 ± 4 Gg/yr) to 71 ± 11 Gg/yr (starting from a prior of 81 ± 29 Gg/yr). The US emission growth rate nevertheless slows down, from +33 %/yr between 1995 and 2000, to +7.5 %/yr between 2000 and 2005, and to +5 %/yr between 2005 and 2010. Until year 2006, our estimates are in excellent agreement with the Environmental Protection Agency EPA estimates (i.e, 54 Gg/yr against 57 Gg/yr respectively for

the year 2004 [US EPA, 2008]. However, our estimated HFC-134a emission increase from 2006 to 2010 contrasts with the decrease suggested by the EPA estimates for these years [US EPA, 2014].

It also should be noted that the posterior emissions show a slight decrease in 2009, also seen by Hu et al., [2015], which is consistent with the decrease of number of vehicles per thousand people (828, [US Transportation 2012]) and with the decrease of fossil fuel CO_2 emissions from transportation [US Energy Information Administration, 2014], probably due to the economic recession. However, this interannual variability for the years 2008-2010 with decrease in 2009 and upwelling in 2010 is not reproduced by the EPA estimates [US EPA, 2014].

3.3.b Europe

The European prior budget is smaller than the US's (68 Gg/yr against 30 Gg/yr in 2005, see Table 2), even though the European number of vehicles is higher (for example, 253 Millions against 275 Millions in 2005 in Europe, estimated with the World Bank http://www.worldbank.org/, and [Davis et al., 2012] data). This can be explained by a higher HFC-134a demand for the mobile air-conditioning sector in the US compared to Europe: when the equipment rate of air-conditioned systems in newer vehicles was 95% for the USA in 1995, it was only 35% for Europe (and then almost 90% in 2005) [Saba et al., 2009; Barbusse et al., 2003]. The US/Europe difference can be also explained by the use in Europe of another gas for the domestic refrigeration, HC600a (isobutane, $(CH_3)_3CH$), which is not used in the US due to flammability issue [Saba et al., 2009].

Our European posterior emissions are in a good agreement with Stohl et al. [2009] and with Reimann et al. [2004] (see Table 4). However, our European budget is twice higher than the

estimates of O'Doherty et al. [2004], with 20 Tg compared to 10 Tg for the years 2000-2002, respectively. However, it should be noted that their study had only benefited from the Mace Head station (compared to the use of the additional JFJ station here).

3.3.c China

Our posterior Chinese emissions of 8 ± 3 Gg/yr (starting from a prior of 8 ± 2 Gg/yr) are higher than the estimates of Yokouchi et al. [2006] for the years 2004-2005, and also significantly higher than the estimates of Yao et al. [2012] for the year 2010 (see Table 4). However, our posterior Chinese estimates of 9 ± 3 Gg/yr (starting from a prior of 9 ± 2 Gg/yr) is similar to the 8.7 Gg/yr (6.5–12) of Kim et al. [2010], and to the 9.8 Gg/yr of Stohl et al. [2009] for year 2005. With a growth rate of 22 %/yr (in agreement with the +20 %/yr obtained by Stohl et al. [2010] between 2005 and 2006), the Chinese emissions reach 11 Gg/yr in 2006.

With a 2005-2010 mean growth rate of +20 %/yr, the Chinese emissions reach 18 Gg/yr in 2008, 40% higher than the 12.9 ± 1.7 Gg estimates of Stohl et al. [2010]. Our Chinese emissions of 20 ± 4 Gg in 2010 are also higher 63% higher than the estimates of Lunt et al., [2015] for this year, derived from a different set of observational constraints (from 8 AGAGE and 2 NIES measurement stations). Nevertheless, our 2010 Chinese value of 20±4 Gg is consistent with the estimates of Su et al., [2015] that suggest about 17 Gg of HFC-134a from mobile air conditioning only, using an improved bottom-up method.

3.3.d Japan

Our Japanese posterior emissions are lower than the prior ones after year 2003, indicating an

overestimation of EDGAR-v4.2 inventory during the period 2004-2010. These posterior emissions are significantly higher than the previous estimates published in the literature. For instance, for the year 2002, we derive posterior Japanese emissions of 11 Gg/yr in 2002 substantially higher than the 4.4 Gg/yr found by Yokouchi et al. [2005]. For 2005 and 2006, we find posterior emissions of 13 ± 4 Gg/yr and 12 Gg/yr for 2005 and 2006 also higher than the 5.3 and 4.0 Gg/yr of Stohl et al. [2009] for the same years. It is worth noting that substantial differences exist between inventory-based quantifications of the Japanese HFC-134a emissions: the EDGARv4.2 inventory estimates the Japanese emissions at 15 ± 8 Gg/yr in 2005, while the UNFCC (United Nations Framework Convention on Climate Change) suggests 3.5 Gg/yr. For their study, Stohl et al. [2009] used the UNFCC**C** inventory as prior, while we use EDGARv4.2. The differences in the choice of prior may be critical, especially if the uncertainty associated to the prior is not well defined and prevents the system from a potentially necessary but important departure from the prior.

3.4 Evaluation against Independent Measurements

To evaluate our posterior HFC-134a US emissions, we compared model simulations with the independent (i.e. not used as constraints in the inversion) HFC-134a measurements from two campaigns: ARCTAS (Arctic Research of the Composition of the Troposphere from Aircraft and Satellites, NASA project, [Barletta et al., 2011]) and CalNex (California Research at the Nexus of Air Quality and Climate Change, [Barletta et al., 2013]). The ARCTAS air samples were obtained on board research flights (DC-8) that flew over California during June 2008. The CalNex 2010 study was performed during May to June 2010. Air samples were collected on board a National Oceanic and Atmospheric Administration (NOAA) WP-3D aircraft. Particular emphasis was

placed on three large source regions - the South Coast Air Basin, the Sacramento Valley, and the San Joaquin Valley - with almost 80% of the samples collected at altitudes below 2 km over the South Coast Air Basin of California (SoCAB) and the Central Valley [Barletta et al., 2013].

We have computed bias and root-mean-square error between the modeled and observed HFC-134a concentrations for each of the 164 and 1125 data, respectively for ARCTAS and CalNex, before and after inversion. On Figure 5, we present ratios between prior and posterior mean bias and root-mean-square error at the grid-cell scale. For bias, ratio has been calculated as:

$$\text{Ratio} = \frac{independentmeasurement - model(beforeinversion)}{independentmeasurements - model(afterinversion)}$$

Grid cells in green, corresponding to a ratio lower than 1, indicate an improvement of the corresponding statistical indicator after optimization.

To further evaluate the interannual variability of our posterior HFC-134a emissions over the long period 1995-2010, we also used cross-validation technique by removing the Niwot Ridge station (from the NOAA network) from the inversion, and we performed an independent evaluation with this site. Figure 8 shows that the inversion leads to a significant improvement relative to the prior simulation. The mean annual reduction of the bias indeed ranges from -13% in 1995 to -80% in 2010, allowing us to confirm that American HFC-134a emissions are overestimated in the EDGAR-v4.2 inventory used here as prior, as seen by Hu et al., [2015]. This overestimation is particularly pronounced after year 2002.

3.5. Seasonality

The 8-day resolution of our inversion reveals seasonal variations in the posterior emissions (which are not present in the prior estimates; see Figure 6 and Figure 7). A seasonal cycle is inferred by the inversion, comparable to the seasonality found by Xiang et al. [2014] and by Hu et al., [2015]. It is

interesting to note that this seasonality is similar to the one found by Fortems-Cheiney et al. [2013] and by Xiang et al. [2014] in HCFC-22 emissions. The seasonal variations of HFC-134a emissions, with higher emissions in summer than in winter, are driven by the US and to a lesser extent by Europe and China. HFC-134a emissions may be exacerbated by higher needs of air conditioning during the warm period and also by extra leaks that occur during the maintenance of cooling systems [Schwarz and Harnisch, 2003].

US emissions exhibit little seasonality prior to 2002 but show an apparent seasonal trend in subsequent years (+4% between January and July 2002, +10% between January and July 2006). This could be explained by i) the increasingly strong signal associated to more than 95% of vehicles equipped with HFC-134a as refrigerant in 2005 [Saba et al., 2009] and/or ii) by the introduction of continuous in situ measurements (i.e, in 2005 at stations Trinidad Head and Ragged Point) and then by the increase of observational constraints that could allow the capture of such a signal.

After 2007 the seasonality of the US emissions becomes strong. For example in 2008, the US August emissions are 26% greater than the January ones (6.44 against 5.12 Gg/month respectively). This results in a slight overestimation of the summer HFC-134a concentrations at NWR station (used for the independent evaluation, see Section 3.4, see Figure 8). Nevertheless, such seasonality is also found by Hu et al. [2015], using different more constrained (with daily flask-air samples and aircraft campaigns) inversion scenarios. They suggested that US summer emissions are 20-50% greater than during winter for the 2008-2012 period.

Conclusions.

We have estimated the spatial and temporal variability of HFC-134a emissions over 16 years, between 1995 and 2010**,** at a 3.75°x2.5° and at 8-day resolution**,** improving our knowledge of the HFC-134a emissions by optimizing both their amplitude and their seasonality.

One of the major findings of this study is the appearance of a seasonal cycle in the HFC-134a emissions in 2002, which becomes enhanced over time. Our results also suggest that the gridded EDGAR-v4.2 inventory overestimates the US and the Japanese budget and confirm the large underestimation of Chinese emissions by this same inventory.

US emissions, and to a lesser extent European emissions, appear to have drastically increased since 1995 (from 10 to 71 Gg/yr in 2010, and from 4 to 37 Gg/yr in 2010, respectively). Driven by these enhancements**,** the global HFC-134a emissions have reached the unprecedented level of 167 ± 5 Gg/yr in 2010.

However, the regional growth rates have slowed down since 1995 over developed countries, with a rate of +5 %/yr for the US, +4 %/yr for Europe and near zero for Japan over 2005-2010. On the contrary, the Chinese emissions, although currently lower than US and European emissions, appear to grow at a rate of +20 %/yr since 2005. Due to the growing demand for vehicles in Asia (269 vehicles per thousand people in 2030 [Davis et al., 2012; WARD, 2010]), the HFC-134a emissions could potentially continue to rise significantly in the near future [Velders et al., 2009; Su et al., 2015], unless this species is phased out by international agreements (e.g, Directive 2006/40/EC of the European Union or North American HFC phase-down amendment proposal [US EPA, 2014]).

Aknowledgements.

We acknowledge the NOAA ESRL, Global Monitoring Division (GMD), Halocarbons and other Atmospheric Trace Species (HATS), the Advanced Global Atmospheric Gases Experiment

(AGAGE), the Italian national Agency for New Technologies, Energy and Sustainable Economic Development (ENEA), and the National Institute for Environmental Studies (NIES) groups for providing HFC-134a measurements, available from the World Data Centre for Greenhouse Gases (http://ds.data.jma.go.jp/gmd/wdcgg/, accessed 15 November 2012), except for the Gosan data. We also thank J.W. Elkins (NOAA), C. Siso (NOAA/CIRES), B. Hall (NOAA), H. Mukai (NIES), A. Disarra (ENEA), S. Piacentino (ENEA) and S. Chiavarini (ENEA). HFC-134a measurements at Gosan are supported by the Korea Meteorological Administration Research and Development Program under Grant CATER 2012-3010, and were provided by S. Li (sun28@snu.ac.kr). We thank S. Barrault (Armines-ParisTech) for the fruitful discussions about the HFC-134a inventories. Finally, we wish to thank F. Marabelle and his team for computer support at LSCE.

References.

Artuso, F., P. Chamard, S. Chiavarini, A. di Sarra, D. Meloni, S. Piacentino, and D. M. Sferlazzo: Tropospheric halocarbons and nitrous oxide monitored at a remote site in the Mediterranean, Atmos. Environ., 44(38), 4944–4953, 2010.

Atkinson, W., J.A. Baker and W. Hill, 2003: Mobile Air Conditioning Industry Overview, SAE Interior Climate Control Standards Committee, Automotive Industry Executive Summit on Vehicle Climate Control, Society of Automotive Engineers (SAE), Troy, MI, USA, February 2003, 24 pp.

Barbusse, S., and Gagnepain, L.: La climatisation automobile, impact énergétique et environnemental, Données et Références ADEME, 2003.

Barletta, B., Nissenson, P., Meinardi, S., Dabdub, D., Sherwood Rowland,F., VanCuren, R.A., Pederson, J., Diskin, G.S., and Blake, D. R.: HFC-152a and HFC-134a emission estimates and characterization of CFCs, CFC replacements, and other halogenated solvents measured during the 2008 ARCTAS campaign (CARB phase) over the South Coast Air Basin of California, Atmos. Chem. Phys., 11, 2655-2669, doi:10.5194/acp-11-2655-2011, 2011.

Barletta, B., et al.: Emission estimates of HCFCs and HFCs in California from the 2010 CalNex study, J. Geophys. Res. Atmos., 118, 2019–2030, doi:10.1002/jgrd.50209, 2013.

Bousquet, P., Hauglustaine, D., Peylin, P., Carouge, C., and Ciais, P.: Two decades of OH variability as inferred by an inversion of atmospheric transport and chemistry of methyl chloroform, Atmos. Chem. Phys, 5,2635-2656, doi:10.5194/acp-5-2635-2005, 2005.

L.J. Carpenter and S. Reimann (Lead Authors), J.B. Burkholder, C. Clerbaux, B.D. Hall, R. Hossaini, J.C. Laube, and S.A. Yvon-Lewis, Ozone-Depleting Substances (ODSs) and Other Gases of Interest tothe Montreal Protocol, Chapter 1in Scientific Assessment of OzoneDepletion: 2014, Global Ozone Research and Monitoring Project –Report No. 55, World Meteorological Organization, Geneva, Switzerland, 2014.

Chevallier, F., Breon, F.-M., and Rayner, P.: The contribution of the Orbiting Carbon Observatory to the estimation of CO_2 sources and sinks: Theoretical study in a variational data assimilation framework, J. Geophys. Res., 112, doi:10.1029/2006JD007375, 2007.

Clodic, D., Baker, J., Chen, J., Hirata, T., Hwang, R., Kohler, J., Peotitjean, C., and Suwono, A.: IPCC/TEAP Special Report. Safeguarding the ozone layer and the global climate system: issues related to hydrofluorocarbons and perfluorocarbons, Cambridge University Press, Cambridge, United Kingdom and New York, NY, USA, 478 pp., 2005.

Clodic, D., Barrault, S. And Saba, S.: Global inventories of the worldwide fleets of refrigerating and air-conditioning equipment in order to determine refrigerant emissions. The 1990 to 2006 updating. ADEME/ARMINES Agreement 0874C0147– Extracts from the Final Report, 2010.

Daniel, J. & G. Velders et al., A Focus on Information and Options for Policymakers, Chapter 5 in Scientific Assessment of Ozone Depletion: 2010, WMO Global Ozone Research and Monitoring Project – Report No. 52, 5.1-5.56, 2011.

Davis, S.C., Diegel, S.W. And Boundy, R.G.: Transportation Energy Data Book, Edition 31 Vehicle Technologies Program, Office of Energy Efficiency and Renewable Energy, U.S. Department of Energy, Contract No. DE-AC05-00OR22725, 2012. Available for download at: cta.ornl.gov/data.

Fortems-Cheiney, A., F. Chevallier, M. Saunois, I. Pison, P. Bousquet, C. Cressot, H. J. Wang, Y. Yokouchi, and F. Artuso (2013), HCFC-22 emissions at global and regional scales between 1995 and 2010: Trends and variability, J. Geophys. Res Atmos., 118, 7379–7388, doi:10.1002/jgrd.50544.

EPA: Direct HFC and PFC Emissions from Use of Refrigeration and Air Conditioning Equipment, Climate Leaders Greenhouse Gas Protocol, EPA430-K-03-004, 2008.

EPA: Text of North American HFC phase-down amendment proposal, http://www.epa.gov/ozone/downloads/HFC_Amendment_2014_Text.pdf, 2014.

Forster, P., V. Ramaswamy, (Coordinating Lead Authors), P. Artaxo, T. Berntsen, R. Betts, D.W. Fahey, J. Haywood, J. Lean, D.C. Lowe, G. Myhre, J. Nganga, R. Prinn, G. Raga, M. Schulz, and R. Van Dorland, Changes in atmospheric constituents and in radiative forcing, Chapter 2 in Climate Change 2007: The Physical Science Basis. Contribution of Working Group I to the Fourth Assessment Report of the Intergovernmental Panel on Climate Change, edited by S. Solomon, D. Qin, M. Manning, Z. Chen, M. Marquis, K.B. Averyt, M. Tignor, and H.L. Miller, 996 pp., Cambridge University Press, Cambridge, U.K., and New York, NY, U.S.A., 2007.

Gilbert, J. and Lemaréchal, C.: Some numerical experiments with variable-storage quasi-Newton algorithms, Math. Programm, 45, 407-435, 1989.

N.R.P. Harris and D.J.Wuebbles (Lead Authors), J.S. Daniel, J. Hu, L.J.M. Kuijpers, K.S. Law, M.J. Prather, and R. Schofield, Scenarios and Information for policymakers, Chapter 5 in Scientific Assessment of Ozone Depletion: 2014, Global Ozone Research and Monitoring Project –Report No. 55, World Meteorological Organization, Geneva, Switzerland, 2014.

Hauglustaine, D. A., Hourdin, F., Jourdain, L., Filiberti, M.-A., Walters, S., Lamarque, J.-F., and Holland, E.: Interactive chemistry in the Laboratoire de Météorologie Dynamique general circulation model: Description and background tropospheric chemistry evaluation, J. Geophys. Res.,

109, doi:10.1029/2003JD003957, 2004.

Hourdin, F., Musat, I., Bony, S., Braconnot, P., and Codron, F.: The LMDZ4 general circulation model : climate performance and sensitivity to parametrized physics with empahsis on tropical convection, Climate Dynamics, 27, pp. 787-813, doi:10.1007/s00382-006-0158-0, 2006.

Hu, J., Wan, D., Li, C., Zhang, J., and Yi, X.: Forecasting of consumption and emission of HFC-134a used in automobile air conditioner sector in China, Adv. Clim. Change Res., 5, 1-6, 2009.

Hu, L., Montzka, S.A., Miller, J.B., Andrews, A.E., Lehman, S.C, Miller, B.R., Thoning, K., Sweeney, C., Chen, H., Godwin, D.S., Masarie, K., Bruhwiler, L., Fischer, M.L., Biraud, S.C, Torn, M.S., Mountain, M., Nehrkorn, T., Eluszkiewicz, J., Miller, S., Draxler, R.R., Stein, A.F., Hall, B.D, Elkins, J.W., and Tans, P.: US emissions of HFC-134a derived for 2008-2012 from an extensive flask-air sampling network, Journal of Geophysical Research-atmospheres, 120, 801-825, doi:10.1002/2014JD022617.

Keller, C.A., Hill, M., Vollmer, M.K., Henne, S., Brunner, D., Reimann, S., O'Doherty, S., Arduini, J., Maione, M., Ferenczi, Z., Haszpra, L., Manning, A.J., and Peter, T.: European emissions of halogenated greenhouses gases inferred from atmospheric measurements, Environ. Sci. Technol., 46, 217-225, dx.doi.org/10.1021/es202453j, 2012.

Kim, J., Li, S., Kim, K.-R. Stohl, A., Muhle, J. M., et al.: Regional atmospheric emissions determined from measurements at Jeju Island: Halogenated compounds from China, Geophys. Res.

Lett., 37, L12801, doi:10.1029/2010GL043263, 2010.

Krol, M. and Lelieveld, J.: Can the variability in tropospheric OH be deduced from measurements of 1,1,1-trichloroethane (methyl chloroform)?, Journal of Geophys. Res., 108, 4125, doi:10.1029/2002JD002423, 2003.

Lunt, M.F, Rigby, M., Ganesan, A.L., Manning, A.J., Prinn, R.G., O' Doherty, S., Muhle, J., Harth, C.M., Salameh, P.K., Arnold, T., Weiss, R.F., Saito, T., Yokouchi, Y., Krummel, P.B., Steele, L.P., Fraser, P.J., Li, S., Park, S., Reimann, S., Vollmer, M.K., Lunder, C., Hermansen, O., Schmidbauer, N., Miaone, M., Arduinin, J., Young, D., and Simmonds, P.G.: Reconciling reported and unreported HFC emissions with atmospheric observations, PNAS, 112, 19, www.pnas.org/cgi/doi/10.1073/pnas.1420247112, 2015.

Manning, A. J. and Weiss, R. F.: Quantifying Regional GHG Emissions from Atmospheric Measurements: HFC-134a at Trinidad Head. 50th Anniversary of the Global Carbon Dioxide Record Symposium and Celebration, Kona, Hawaii, Available for download at: http://www.esrl.noaa.gov/gmd/co2conference/pdfs/, 2007.

Millet, D. B., Atlas, E. L., Blake, D. R., Blake, N. J., Diskin, G. S., et al. (2009): Halocarbon emissions from the United States and Mexico and their Global Warming Potential, Environ. Sci. Technol., 43, 1055–1060, 2009.

Molina, M., Zaelke, D., Sarma, K. M., Andersen, S. O., Ramanathan, V., and Kaniaru, D.:

Reducing abrupt climate change risk using the Montreal Protocol and other regulatory actions to complement cuts in CO2 emissions, Proc. Natl. Acad. Sci. USA, Early Edition, http://www.pnas.org/content/early/2009/10/09/0902568106.full.pdf, 2009.

Montzka, S.A., Myers, R.C., Butler, J.H., Elkins, J.W., Lock, L.T., Clarke, A.D. And Goldstein, A.H.: Observations of HFC-134a in the remote troposphere, Geophys. Res. Lett., 23, 2, DOI: 10.1029/95GL03590, 1996.

Montzka, S.A. And Reimann, S. (Coordinating Lead Authors), Engel, A., Hruger, K., O'Doherty, S., Sturges, W.T., Blake, D., Dorf, M., Fraser, P., Froidevaux, L., Jucks, K., Kreher, K., Kurylo, M.J., Mellouki, A., Miller, J., Nielsen, O.-J., Orkin, V.L., Prinn, R.G., Rhew, R., Santee, M.L., Stohl, A. and Verdonik, D., Ozone-Depleting Substances (ODSs) and Related Chemicals , Chapter 1 in Scientific Assessment of Ozone Depletion: 2010, Global Ozone Research and Monitoring Project-Report No. 52, 516 pp., World Meteorological Organization, Geneva, Switzerland, 2011.

Montzka, S.A., McFarland, M., Andersen, S.O., Miller, B.R., Fahey, D.W., Hall, B.D., Hu, L., Siso, C. And Elkins, J.W.: Recent trands in global emissions of hydrochlorofluorocarbons and hydrofluorocarbons: Reflecting on the 2007 adjustments to the Montreal Protocol, Journal of Physical Chemistry A, 119, 4439-4449, 2014.

O'Doherty, S., D.M. Cunnold, A. Manning, B.R. Miller, R.H.J. Wang, P.B. Krummel, P.J. Fraser, P.G. Simmonds, A. McCulloch, R.F. Weiss, P. Salameh, L.W. Porter, R.G. Prinn, J. Huang, G.

Sturrock, D. Ryall, R.G. Derwent and S.A. Montzka, Rapid growth of HFC-134a, HCFC-141b, HCFC-142b and HCFC-22 from AGAGE observations at Cape Grim, Tasmania and Mace Head, Ireland, J. Geophys. Res., 109, D06310, doi:10.1029/2003JD004277, 2004.

Papasavva, S., Luecken, D. J., Waterland, R. L., Taddonio, K. N., and Andersen, S. O.: Estimated 2017 refrigerant emissions of 2,3,3,3-tetrafluoropropene (HFC-1234yf) in the United States resulting from automobile air conditioning, Environ. Sci. Technol., 43, 9252–9259, 2009.

Prinn, R.G., R.F. Weiss, P.J. Fraser, P.G. Simmonds, D.M. Cunnold, F.N. Alyea, S. O'Doherty, P. Salameh, B.R. Miller, J. Huang, R.H.J. Wang, D.E. Hartley, C. Harth, L.P. Steele, G. Sturrock, P.M. Midgley, and A. McCulloch, A history of chemically and radiatively important gases in air deduced from ALE/GAGE/AGAGE, J. Geophys. Res., 115, 17751-17792, 2000.

Prinn, R.G., Huang, J., Weiss, R.F., Cunnold, D.M., Fraser, P., Simmonds, P.G., McCulloch, A., Harth, C., Salameh, P., ODoherty, S., Wang, R. H.J., Porter, L., and Miller, B.R.: Evidence for substantial variations of atmospheric hydroxyl radicals in the past two decades, Science, 292, 1882-1888, 2001.

Reimann, S., Schaub, D., Stemmler, K., Folini, D., Hill, M., Hofer, P., Buchmann, B., Simmonds, P. G., Greally, B. R., and O'Doherty, S.: Halogenated greenhouse gases at the Swiss high alpine site of Jungfraujoch (3580 m asl): Continuous measurements and their use for regional European source allocation, J. Geophys. Res., 109, D05307, doi:10.1029/2003JD003923, 2004.

Rigby, M., Prinn, R.G., O'Doherty, S., Miller, B.R., Ivy, D., Mulhe, J., Hart, C.M., Salameh, P.K., Arnold, T., Weiss, R.F., Krummel, P.B., Steele, L.P., Fraser, P.J., Young, D. And Simmonds, P.G.: Recent and future trends in synthetic greenhouse gas radiative forcing, Geophysical Research Letters, 41 2623-2630, doi:10.1002/2013GL059099, 2014.

Rugh, J., V. Hovland and S.O. Andersen, 2004: Significant Fuel Savings and Emission Reductions by Improving Vehicle Air Conditioning. Proceedings of the Mobile Air Conditioning Summit 2004, 15 April 2004, Washington, DC, USA. Earth Technologies Forum, Arlington, VA, USA.

Saba, S., Slim, R., Palandre, L. And Clodic, D.: Inventory of direct and indirect GHG emissions from stationary air conditioning and refrigeration sources, with special emphasis on retail food refrigeration and unitary air conditioning. Final Report for CARB, 2009.

Sander, S. P., et al. (2011), Chemical Kinetics and Photochemical Data for Use in Atmospheric Studies, Evaluation No. 17, JPL Publication 10-6, Jet Propulsion Laboratory, Pasadena, http://jpldataeval.jpl.nasa.gov.

Schwarz, W. and J. Harnisch (2003) Establishing the Leakage Rates of Mobile Air Conditioners; Study carried out for DG Environment of the European Commission. Brussels. 17 April 2003. Contract number B4-3040/2002/337136/MAR/C1. Available for download at: http://www.europa.eu.int/comm/environment/climat/pdf/leakage_rates_final_report.pdf

Stohl, A., Seibert, P., Arduini, J., Eckhardt, S., Fraser, P., Greally, B.R., Lunder, C., Maione, M.,

Muhle, J., O'Doherty, S., Prinn, R.G., Reimann, S., Saito, T., Schmidbauer, N., Simmonds, P.G., Vollmer, M.K., Weiss, R.F. and Yokouchi, Y: An analytical inversion method for determining regional and global emissions of greenhouse gases: Sensitivity studies and application to halocarbons, Atmos. Chem. Phys., 9, 1597-1620, 2009.

Stohl, A., J. Kim, S. Li, S. O'Doherty, J. Mhle, P. K. Salameh, T. Saito, M. K. Vollmer, D. Wan, R. F. Weiss, B. Yao, Y. Yokouchi, and L. X. Zhou: Hydrochlorofluorocarbon and hydrofluorocarbon emissions in East Asia determined by inverse modeling. Atmos. Chem. Phys, 10, 3545-3560, 2010.

Kuijpers, L.: Technical Options Committee Refrigeration, A/C and Heat Pumps Assessment Report, ISBN 978-9966-20-002-0, 2011.

Su, S., Fang, X., Li, L., Wu, J., Zhang, J., Xu, W., and Hu, J. : HFC-134a emissions from mobile air conditioning in China from 1995 to 2030, Atmospheric Environment, 102, 122-129, 2015.

US Department of Transportation, Federal Highway Administration, Highway Statistics 2010, Washington, DC, 2012.

US Energy Information Administration, Monthly Energy Review Rep. DOE/EIA-0035(2014/01), 2014.

Velders, G. J. M., Fahey, D. W., Daniel, J. S., McFarland, M., and Andersen, S. O.: The large

contribution of projected HFC emissions to future climate forcing, Proc. Natl. Acad. Soc., 106, 10949-10954, 2009.

WARD, Ward's Communications, Ward's Motor Vehicle Data, 287-290, 2010.

Wallington, J., Sullivan, J.L., and Hurley, M.D.: Emissions of CO_2, CO, NO_x, HC, PM, HFC-134a, N_2O and CH_4 from the global light duty vehicle fleet, Meteorologische Zeitschrift, Vol. 17, No. 2, 109-116, 2008.

Wimberger, E.: Emissions of HFC-134a in Auto Dismantling and Recycling. Report prepared for the State of California Air Resources Board, Contract Number 06-334, revised on 16 July, 2010.

Xiang, B., Patra, P.K., Montzka, S.A., Miller, S.M., Elkins, J.W., Moore, F.L., Atlas, E.L., Miller, B.R., Weiss, R.F., Prinn, R.G., and Wofsy, S.C.: Global emissions of refrigerants HCFC-22 and HFC-134a: Unforeseen seasonal contributions, PNAS, 111,49,17379-17384, 2014.

Yao, B., Vollmer, M. K., Zhou, L.X., Henne, S., Reimann, S., Li, P. C., Wenger, A., and Hill, M.: In-situ measurements of atmospheric hydrofluorocarbons (HFCs) and perfluorocarbons (PFCs) at the Shangdianzi regional background station, China, Atmos. Chem. Phys., 12, 10181-10193, doi:10.5194/acp-12-10181-2012, 2012.

Yokouchi, Y., Inagaki, T., Yazawa, K., Tamaru, T., Enomoto, T., and Izumi, K.: Estimates of ratios

of anthropogenic halocarbon emissions from Japan based on aircraft monitoring over Sagami Bay, Japan, Journal of Geophysical Research-Atmospheres, 110, D06301, 2005.

Yokouchi, Y., Taguchi, S., Saito, T., Tohjima, Y., Tanimoto, H. And Mukai, H.: high-frequency measurements of HFCs at a remote site in East Asia and their implications for Chinese emissions, Geophys. Res.Lett, 33, L21814, doi:10.1029/2006GL026403, 2006.

	USA		Europe		Japan		China		Globe	
	Prior	**Post**	Prior	**Post**	Prior	**Post**	Prior	**Post**	Prior	**Post**
1995	10±4	**10±2**	4±1	**4±1**	4±1	**2±1**	<1	**<1**	20±4	**18±2**
1996	16	**17**	7	**7**	4	**4**	<1	**<1**	33	**33**
1997	22	**23**	9	**9**	5	**6**	<1	**<1**	43	**44**
1998	29	**31**	12	**13**	7	**8**	<1	**<1**	55	**60**
1999	37	**35**	15	**16**	8	**9**	<1	**<1**	71	**70**
2000	44	**36**	18	**18**	10	**10**	2	**2**	86	**78**
2001	50	**42**	21	**20**	11	**11**	2	**2**	98	**89**
2002	55	**47**	23	**23**	12	**12**	3	**3**	109	**102**
2003	59	**50**	26	**25**	13	**13**	5	**5**	121	**110**
2004	64	**54**	29	**28**	14	**12**	7	**7**	133	**119**
2005	68±24	**57±9**	30±9	**29±5**	15±8	**13±4**	9±3	**9±2**	145±29	**128±5**
2006	73	**55**	33	**30**	16	**12**	12	**11**	157	**130**
2007	77	**61**	35	**31**	16	**12**	15	**14**	170	**138**
2008	81	**60**	37	**34**	17	**12**	20	**18**	183	**147**
2009	81	**59**	37	**34**	17	**11**	20	**18**	183	**147**
2010	81±29	**71±11**	36±11	**37±6**	17±11	**12±2**	21±8	**20±4**	183±34	**167±5**

Table 1. Global and regional HFC-134a emissions before the inversion (prior) and after the inversion (posterior) in Gg/yr over the period 1995-2010. As a trade off between computing resources and completeness, we only estimate the posterior one-sigma uncertainty for the years 1995, 2005 and 2010.

Station	Code	Latitude (in °)	Longitude (in °)	Altitude (m.a.s.l)	Network	Type	Sampling Frequency	Data Period
Alert, Canada	ALT	82.50	-62.30	210	NOAA	flask	weekly	12/1994-03/2011
Pt. Barrow, AK, USA	BRW	71.30	-156.60	11	NOAA	flask	weekly	12/1994-03/2011
Cape Grim, Tasmania	CGO	-40.68	144.68	104	AGAGE	continuous	hourly	01/1998-03/2011
Cape Grim, Tasmania	CGO	-40.68	144.68	21	NOAA	flask	weekly	12/1994-03/2011
Cape Ochi-ishi, Japan	COI	43.15	145.50	96	NIES	continuous	hourly	08/2006-12/2010
Gosan, Republic of Korea	GOS	33.17	126.90	46.5	AGAGE	continuous	hourly	11/2007-03/2011
Hateruma, Japan	HAT	24.05	123.80	46.5	NIES	continuous	hourly	05/2004-12/2010
Harvard Forest, USA	HFM	42.90	-72.30	340	NOAA	flask	weekly	11/1995-03/2011
Jungfraujoch, Switzerland	JFJ	46.54	7.98	3580	AGAGE	continuous	hourly	01/2000-03/2011
Cape Kumakahi, HI, USA	KUM	19.52	-154.82	3	NOAA	flask	weekly	11/1995-03/2011
Park Falls, WI, USA	LEF	45.92	-90.27	868	NOAA	flask	weekly	10/1996-03/2011
Lampedusa, Italy	LMP	35.52	12.63	45	ENEA	flask	weekly	12/2003-12/2008

Mace Head, Ireland	MHD	53.33	-9.90	25	AGAGE	continuous	hourly	12/1994-03/2011
Mace Head, Ireland	MHD	53.33	-9.90	8	NOAA	flask	weekly	10/1998-03/2011
Mauna Loa, USA	MLO	19.54	-155.58	3397	NOAA	flask	weekly	12/1994-03/2011
Palmer Station, Antarctica	PSA	-64.92	-64.00	10	NOAA	flask	weekly	12/1997-03/2011
Ragged Point, Barbados	RPB	13.17	-59.43	42	AGAGE	continuous	hourly	05/2005-03/2011
Cape Matatula, Samoa	SMO	-14.24	-170.57	77	AGAGE	continuous	hourly	05/2006-03/2011
Cape Matatula, Samoa	SMO	-14.24	-170.57	42	NOAA	Flask	weekly	12/1994-03/2011
South Pole, USA	SPO	-89.98	-24.80	2810	NOAA	flask	weekly	12/1994-03/2011
Summit, Greenland	SUM	72.58	-38.48	3238	NOAA	flask	weekly	06/2004-03/2011
Tierra del Fuego, Argentina	TDF	-54.87	-68.48	20	NOAA	flask	weekly	05/2004-05/2010

Trinidad Head, CA, USA	THD	41.05	-124.15	120	NOAA	flask	weekly	03/2002-03/2011
Trinidad Head, CA, USA	THD	41.05	-124.15	140	AGAGE	continuous	hourly	03/2005-03/2011
Ny-Alesund, Norway	ZEP	78.90	11.88	474	AGAGE	continuous	hourly	01/2001-03/2011

Table 2. List of the stations performing HFC-134a measurements used in this study. See Figure 2 for the station locations. The data period listed is specific to this study. The different networks are the National Oceanic and Atmospheric Administration, Earth System Research Laboratory NOAA/ESRL, the Advanced Global Atmospheric Gases Experiment AGAGE, the National Institute for Environmental Studies NIES, and the Italian national Agency for New Technologies, Energy and Sustainable Economic Development ENEA. The AGAGE data are two-hourly for the newer Medusa-GCMS measurements, and 4-hourly for the older ADS-MS measurements.

	USA	Europe	Japan	China	Globe
1995	54	-	11	-	56
2005	56	45	40	23	71
2010	61	45	80	46	84

Table 3. Regional and global uncertainty reductions in %, for the years 1995, 2005 and 2010.

Globe	**Literature**	**This work**
1996	20 [Xiang et al., 2014]	**17**
2007–2009	141.6 [Lunt et al., 2015]	**144**
2010	153 [Xiang et al., 2014]	**167**
US		
2004	27 *[Millet et al., 2009]*	**54**
2005	35 *[Stohl et al., 2009]*	**57**
2006	43 *[Manning and Weiss, 2007]*	**55**
2008	43±6 *[Barletta et al., 2011]*	**60**
2008	53–70 *[Hu et al., 2015]*	**60**
2009	47–60 *[Hu et al., 2015]*	**59**
2010	54–68 *[Hu et al., 2015]*	**71**
Europe		
2000-2002	23.6 [Reimann et al., 2004]	**20**
2000-2002	10 *[O'Doherty et al., 2004]*	**20**
2005	24 *[Stohl et al., 2009]*	**29**
2006	27 *[Stohl et al., 2009]*	**30**
China		
2004-2005	3.9±2.4 *[Yokouchi et al., 2006]*	**8**
2005	8.7 *[Kim et al., 2010]* 9.8 *[Stohl et al., 2009]*	**9**

2010	6±5.6 *[Yao et al., 2012]*	**21**
Japan		
2002	4.4 *[Yokouchi et al., 2006]*	**11**
2005	5.3 *[Stohl et al., 2009]*	**13**
2006	4 *[Stohl et al., 2009]*	**12**

Table 4. *Comparison with previous published annual total budgets for the period 1995-2010 studied here.*

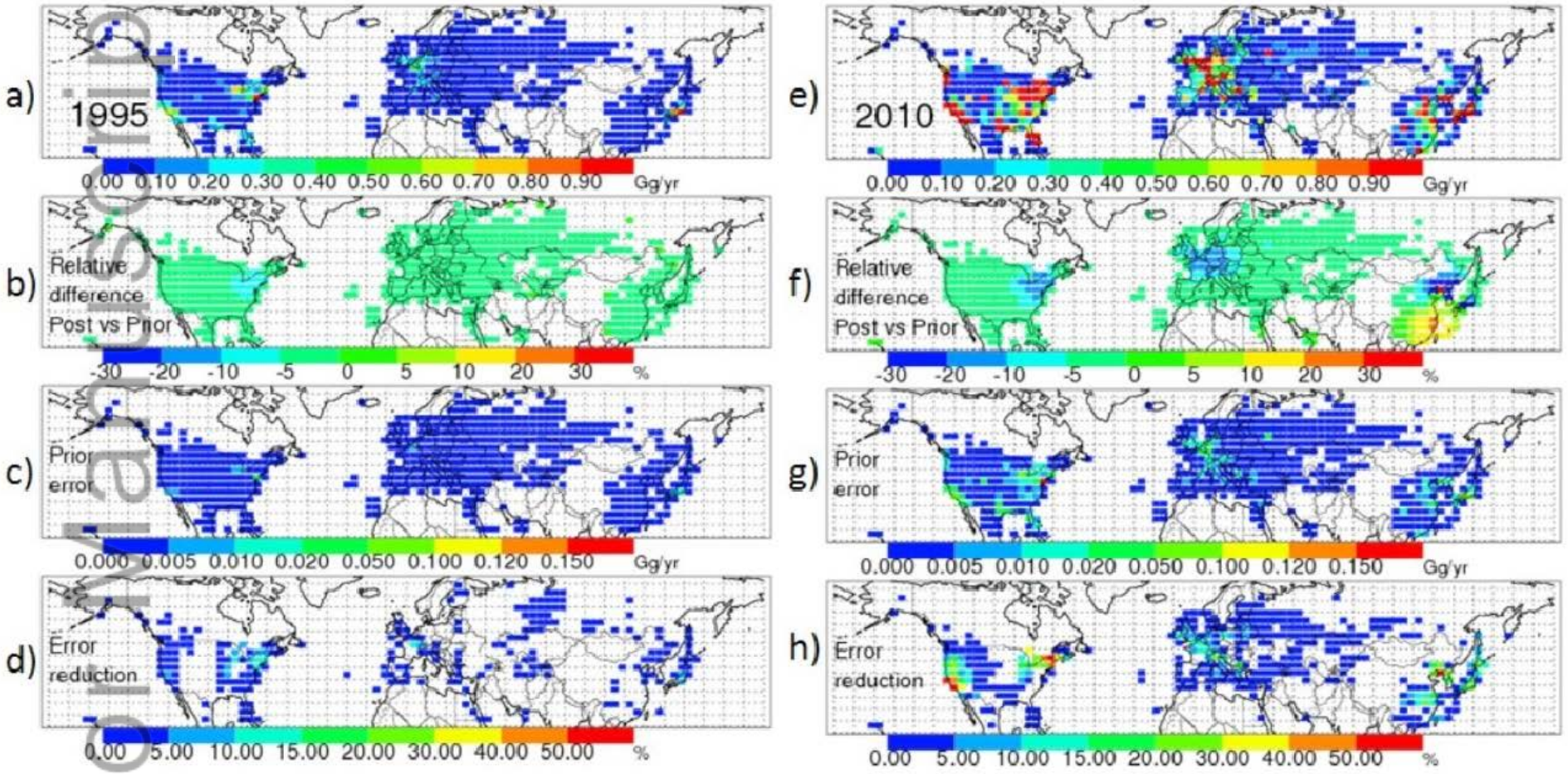

Figure 1. left) a) Grid-point prior HFC-134a emissions in Gg/yr for year 1995. b) Relative difference between posterior and prior emissions in %. c)

Prior uncertainty in Gg/yr. d) Uncertainty reduction at the grid-point resolution, in %. **right)** same as left, but for year 2010.

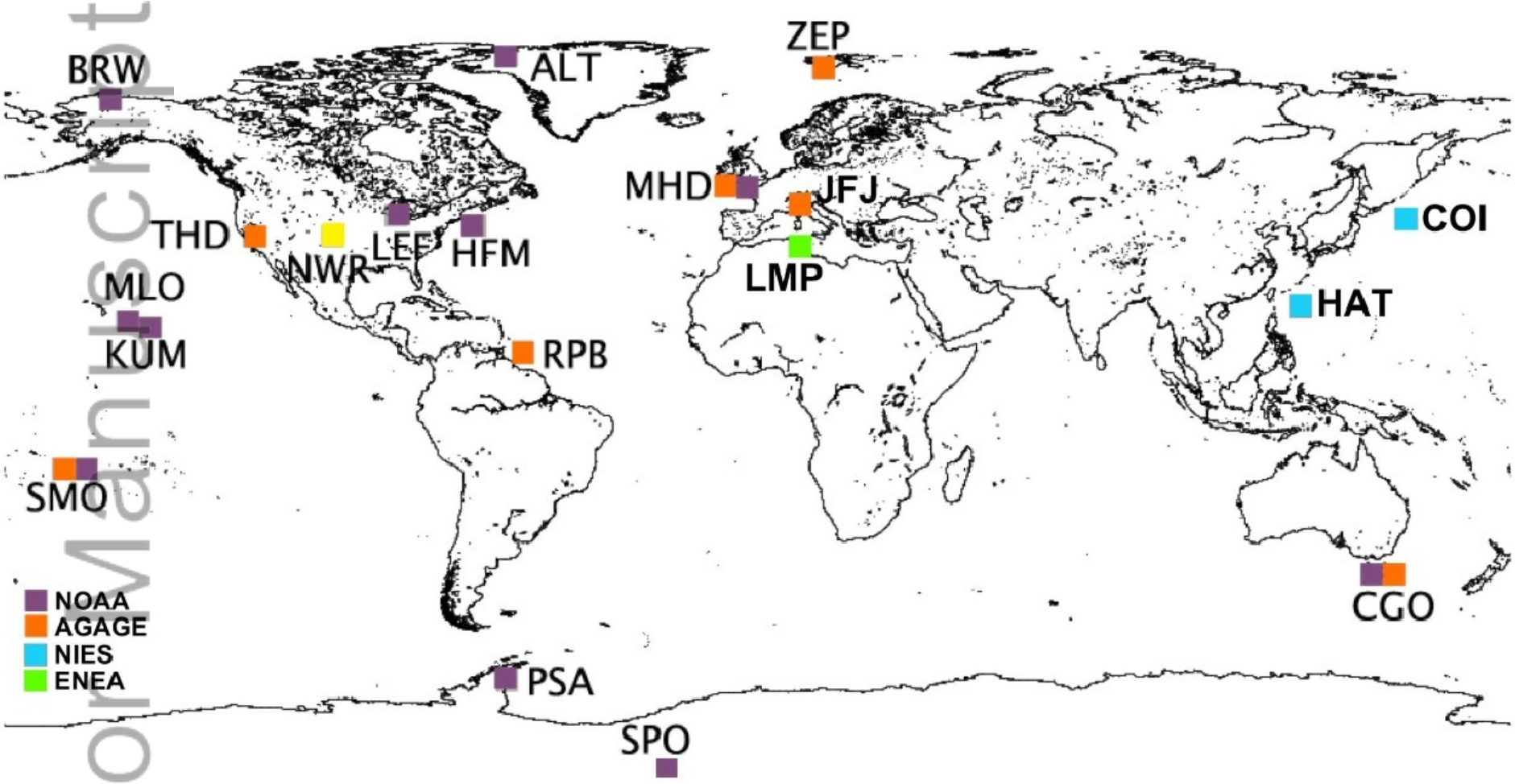

Figure 2. Locations of the stations measuring HFC-134a dry air mole fractions used in the inversion. The measurements of the Niwot Ridge station (NWR, USA) displayed in yellow are only used for the evaluation.

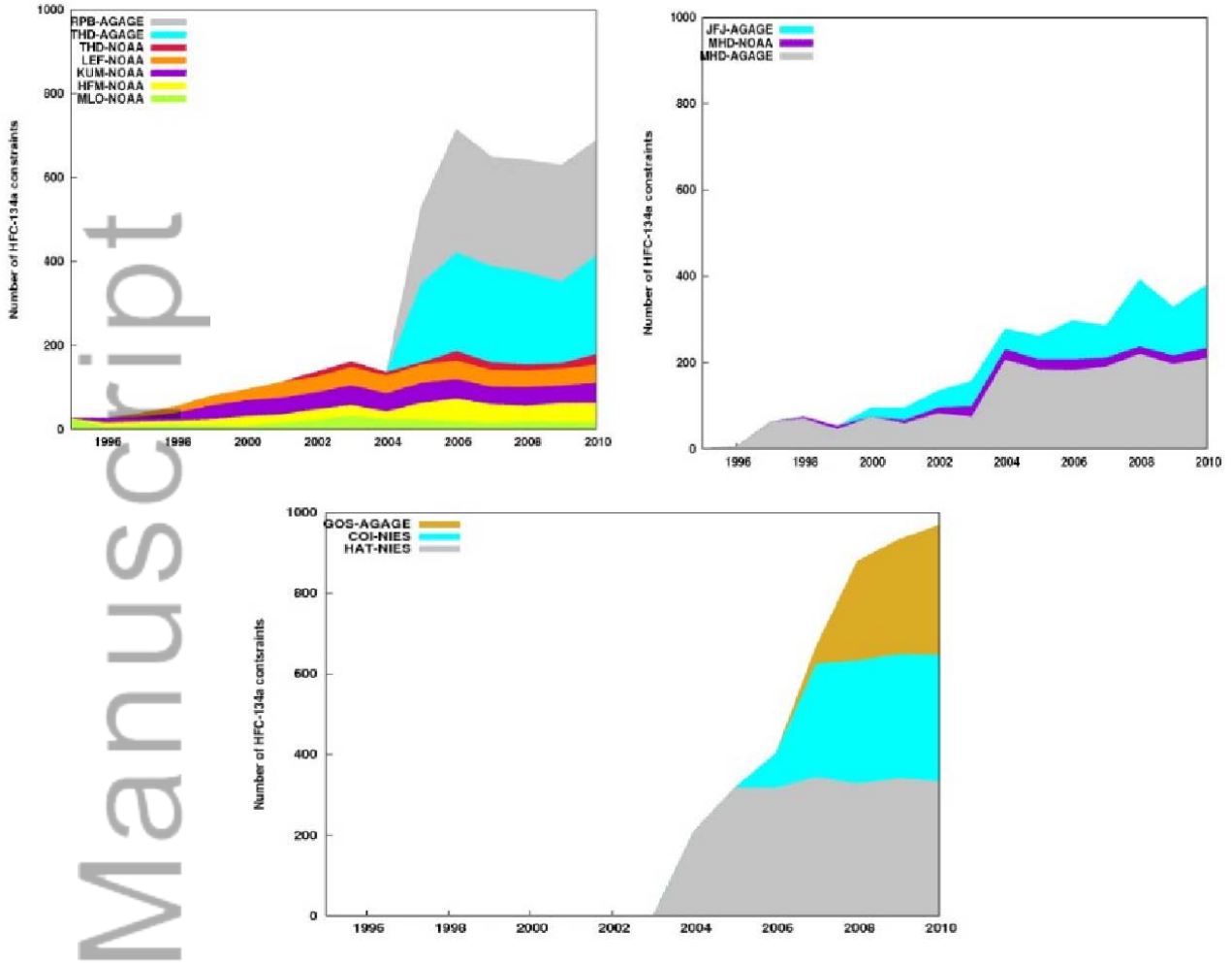

Figure 3. Total number of HFC-134a constraints used in the inversion system per year for a) the US, b) Europe and c) China. See Figure 2 for the locations of the stations.

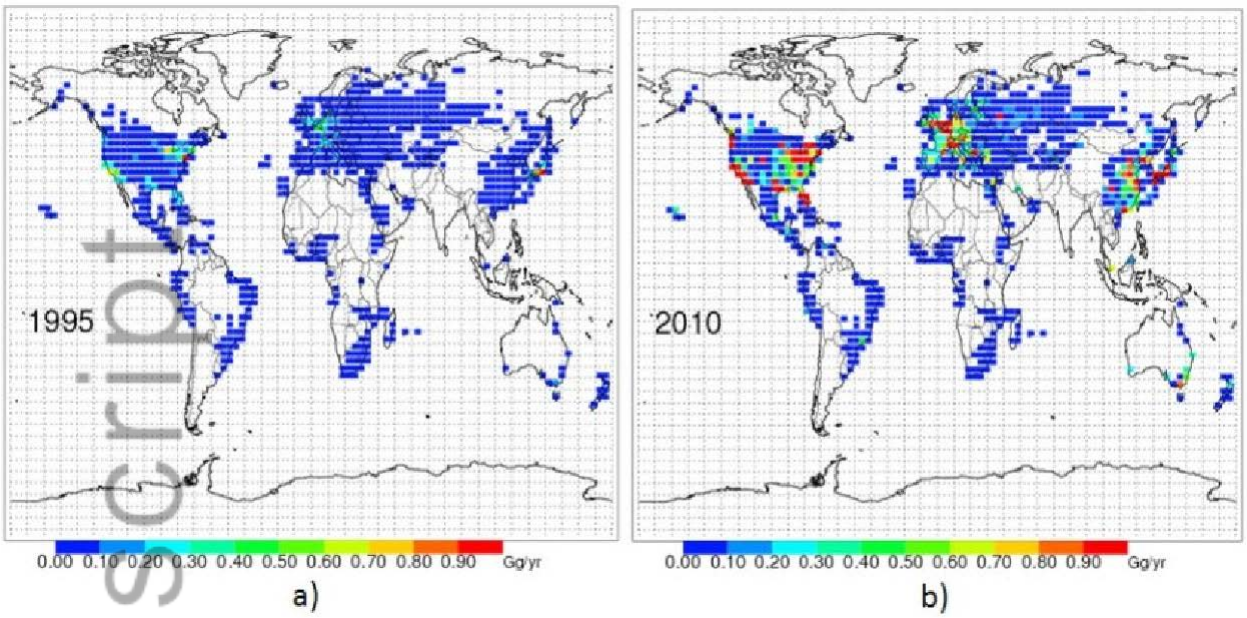

Figure 4. Grid-point global posterior HFC-134a emissions in Gg/yr for a) year 1995 and b) year 2010.

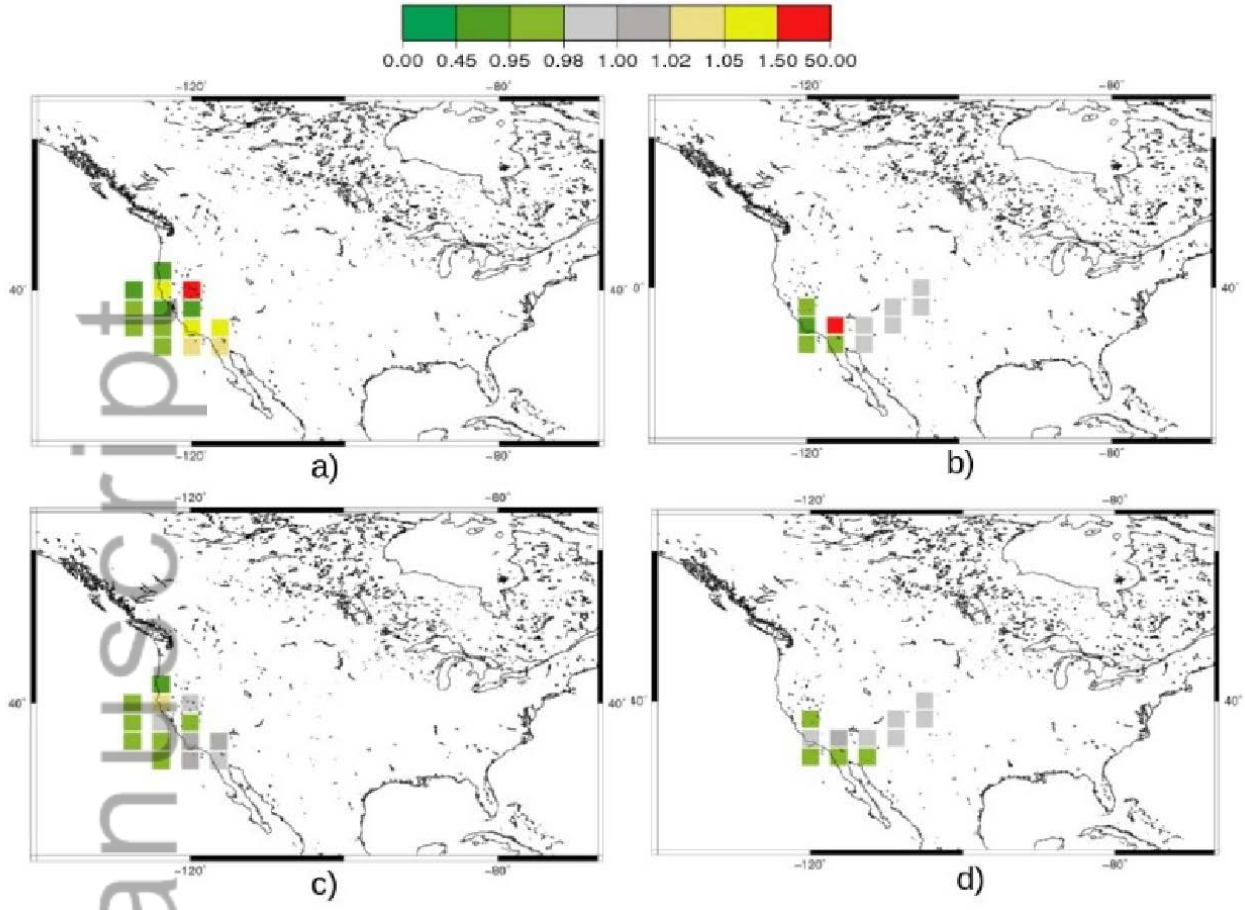

Figure 5. Ratio of the posterior to the prior values of the bias (in absolute value) between simulated and observed concentrations for a) ARCTAS (flying in June 2008), and b) CalNex (flying in May-June 2010) campaigns. Ratio of the posterior to the prior values of the root-mean-square error between simulated and observed concentrations for c) ARCTAS and d) CalNex. The inversion improves the simulation when the ratios are less than 1 (in green).

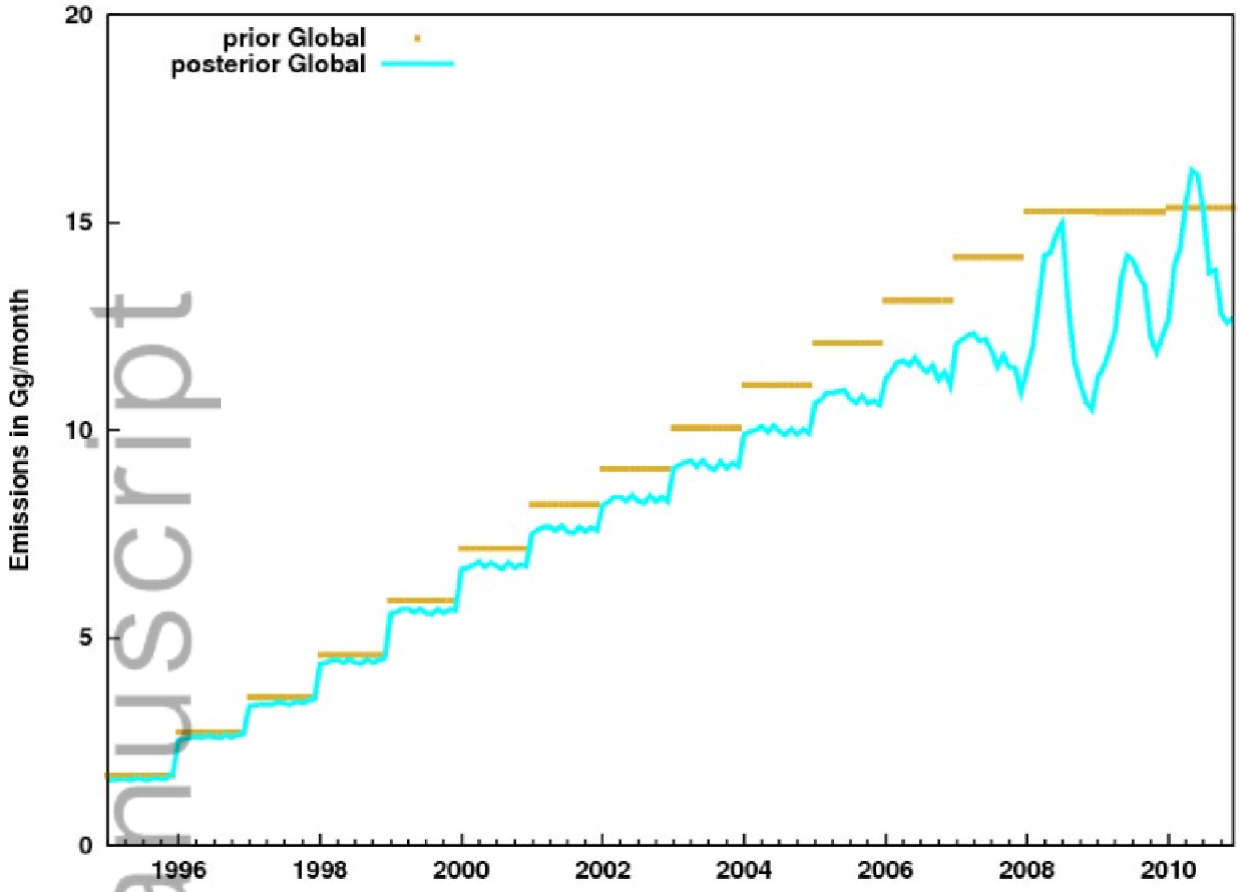

Figure 6. Global monthly HFC-134a prior and posterior emissions (in yellow and blue), from 1995 to 2010, in Gg/month.

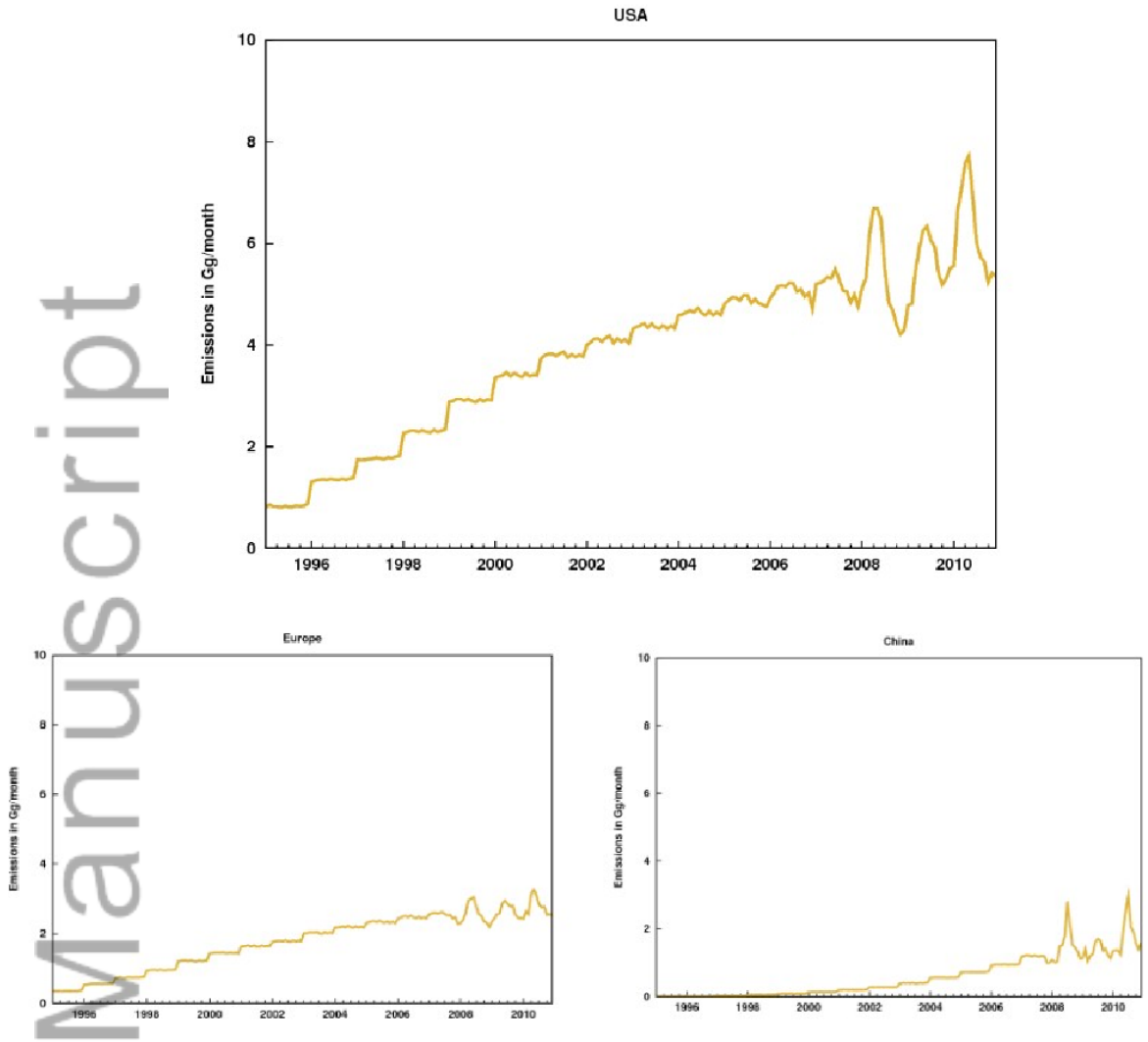

Figure 7. HFC-134a posterior emissions from 1995 to 2010, for the US, Europe and China, in Gg/month.

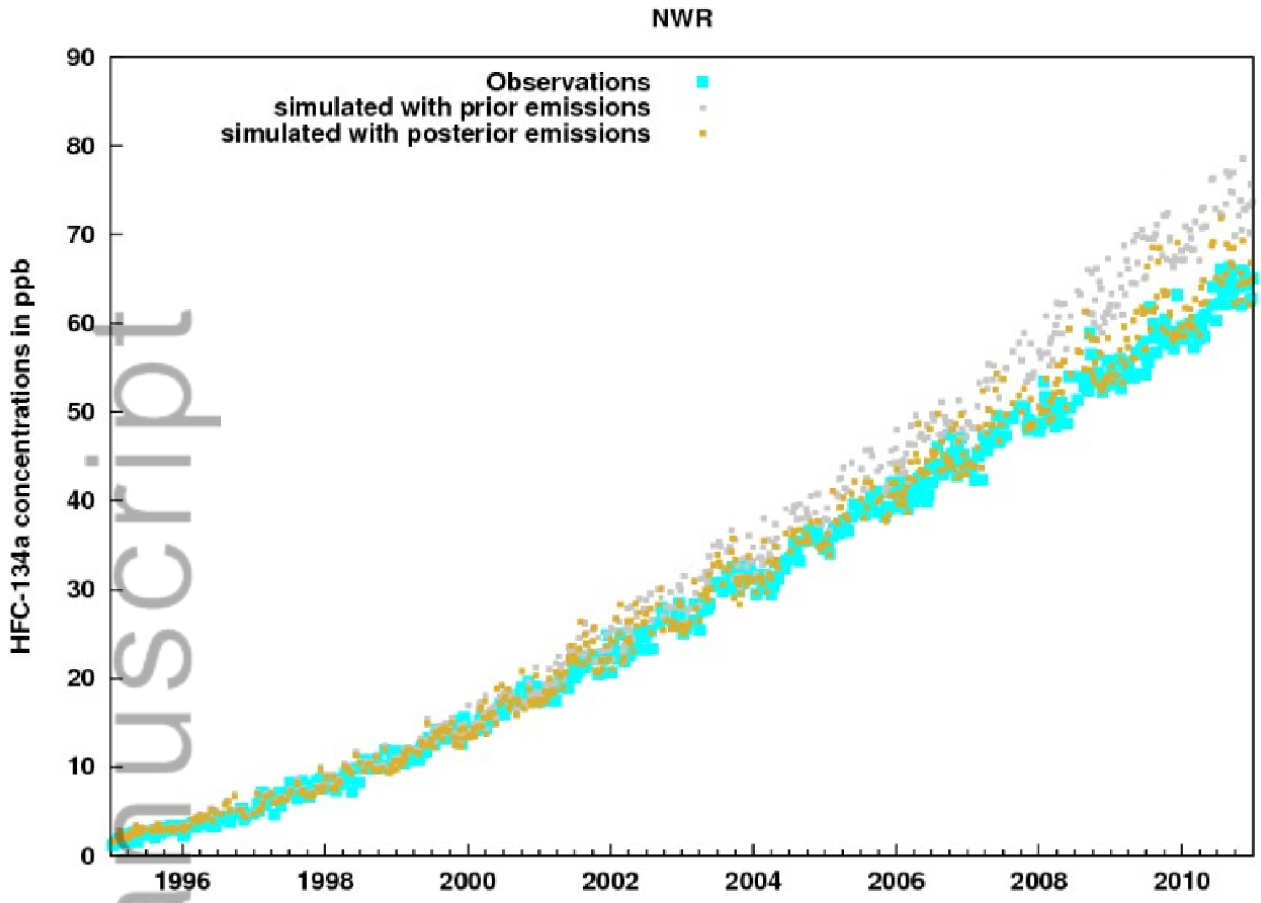

Figure 8. Simulated prior (grey) and posterior (yellow) compared to the measured (blue) HFC-134a concentrations at station Niwot Ridge (USA, Colorado). See Figure 2 for the station location. The mean annual reduction of the bias indeed ranges from -13% in 1995 to -80% in 2010.

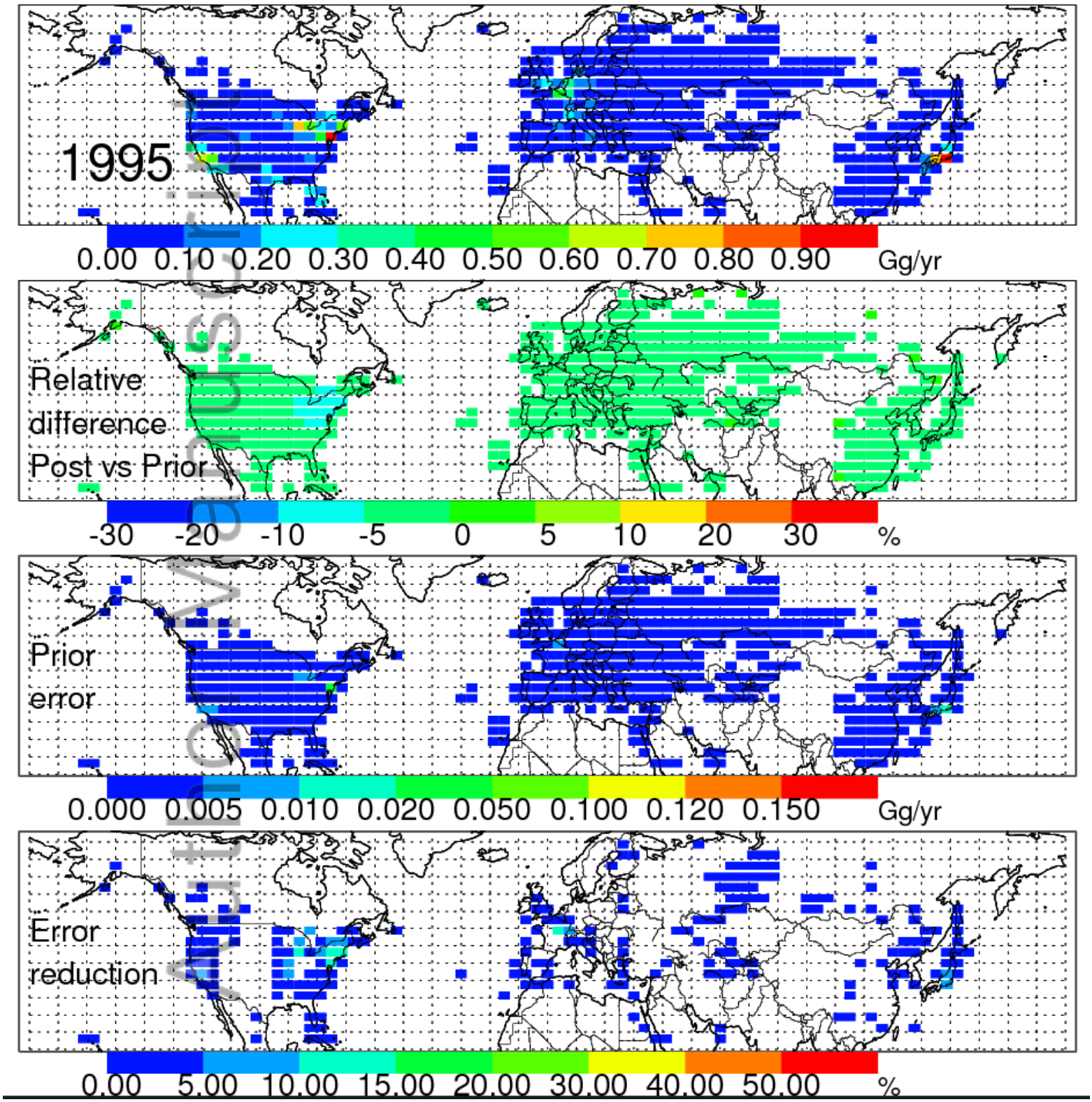

2015JD023741-f01-z-4c.png

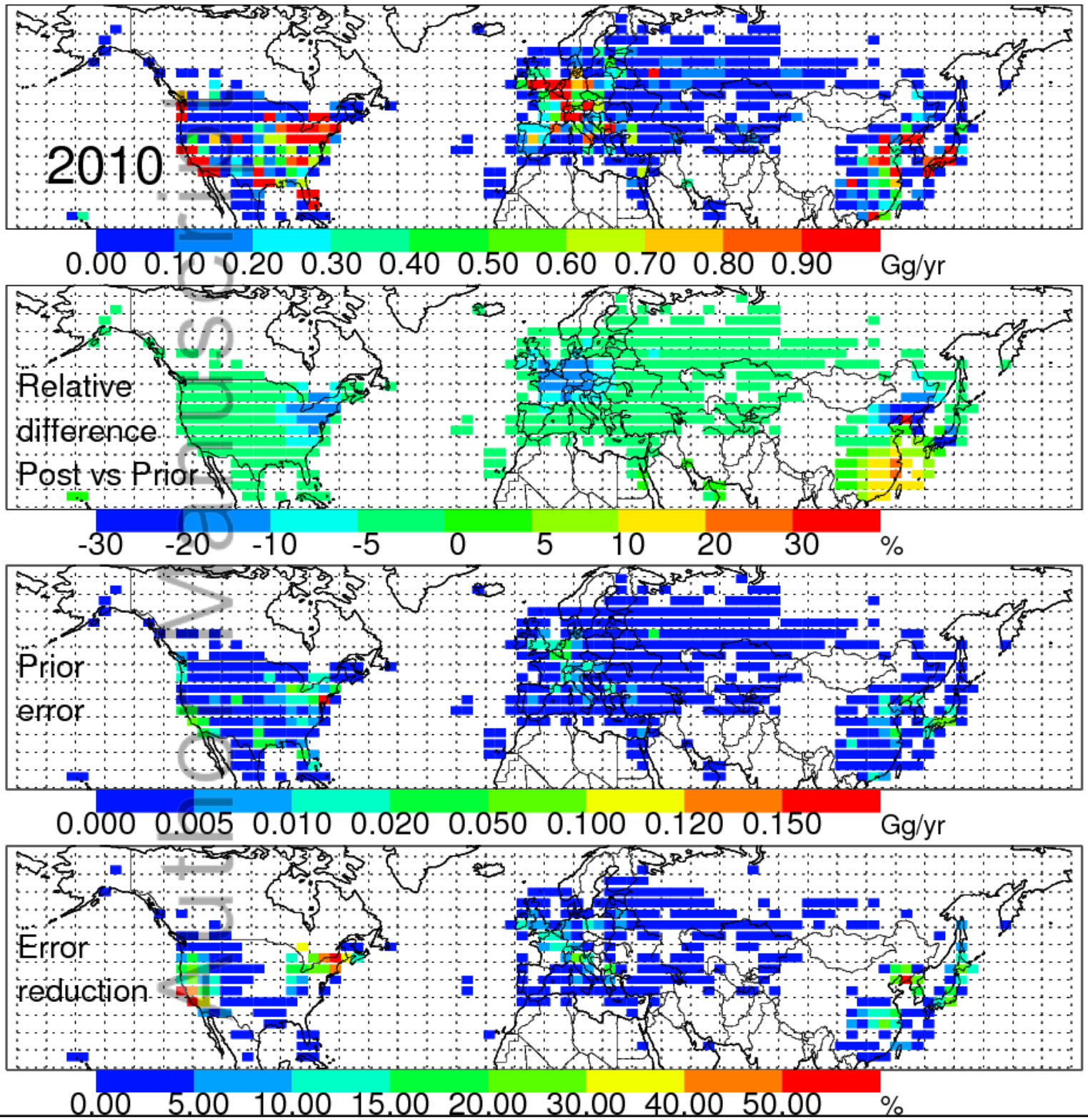

2015JD023741-f02-z-4c.png

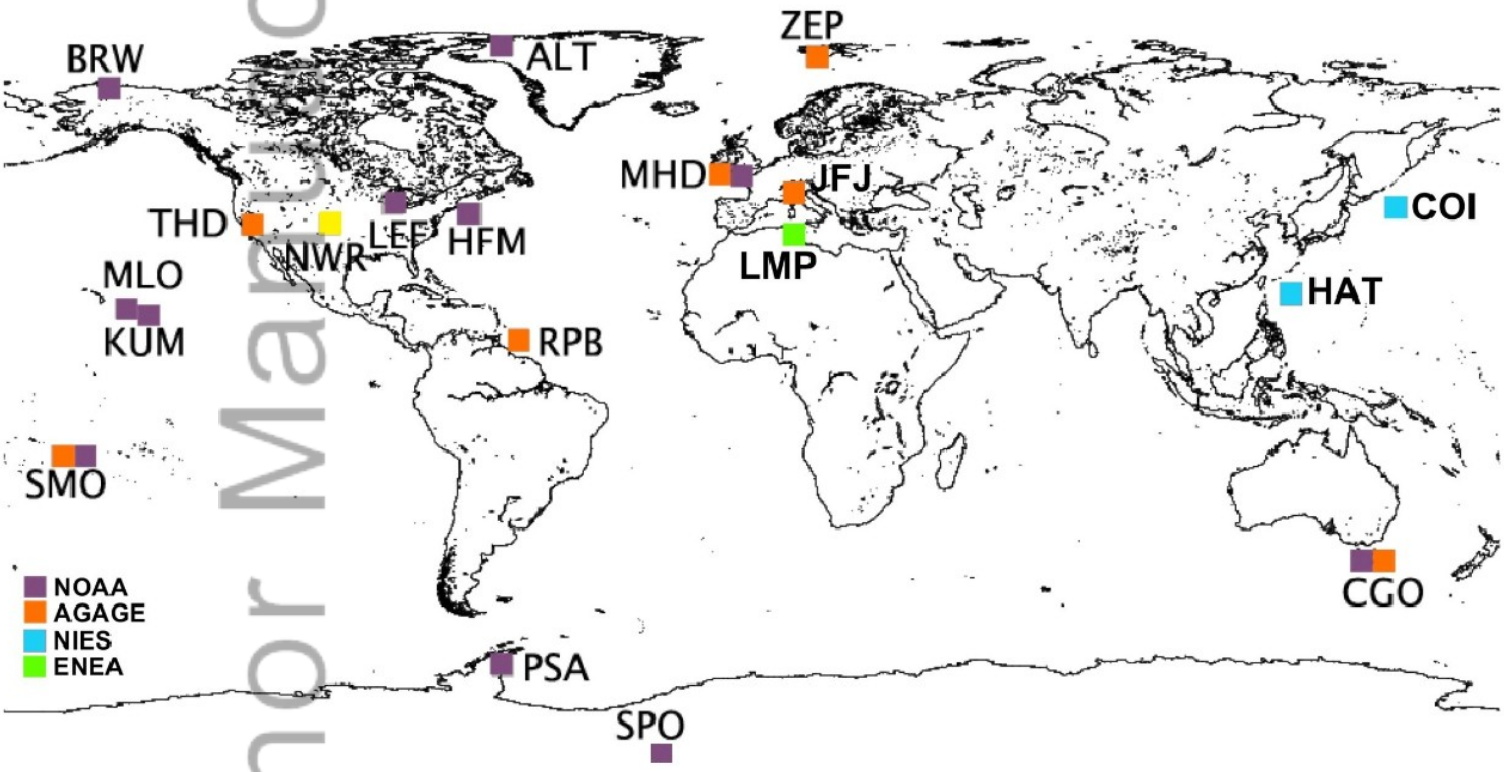

2015JD023741-f03-z-4c.png

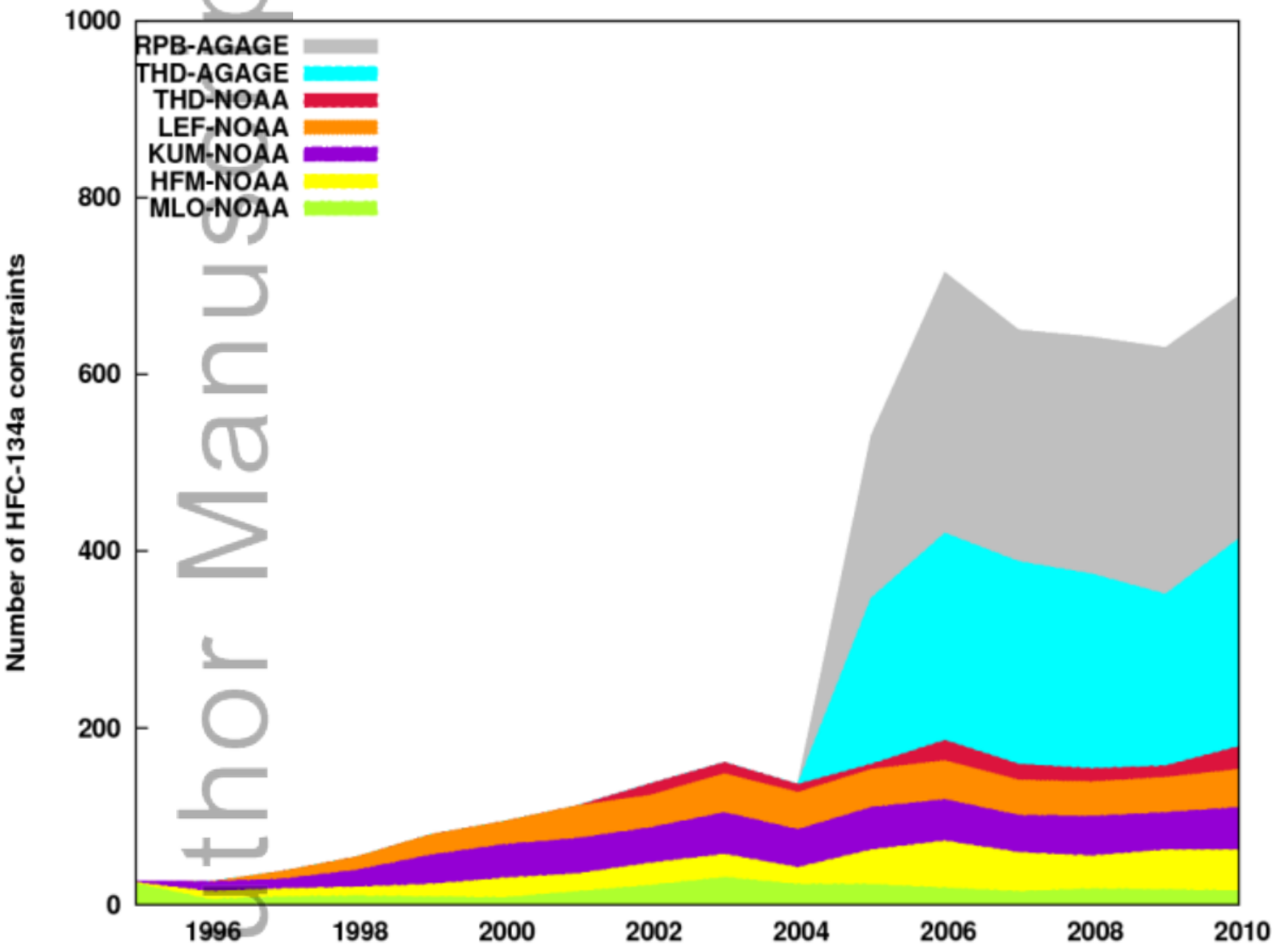

2015JD023741-f04-z-4c.png

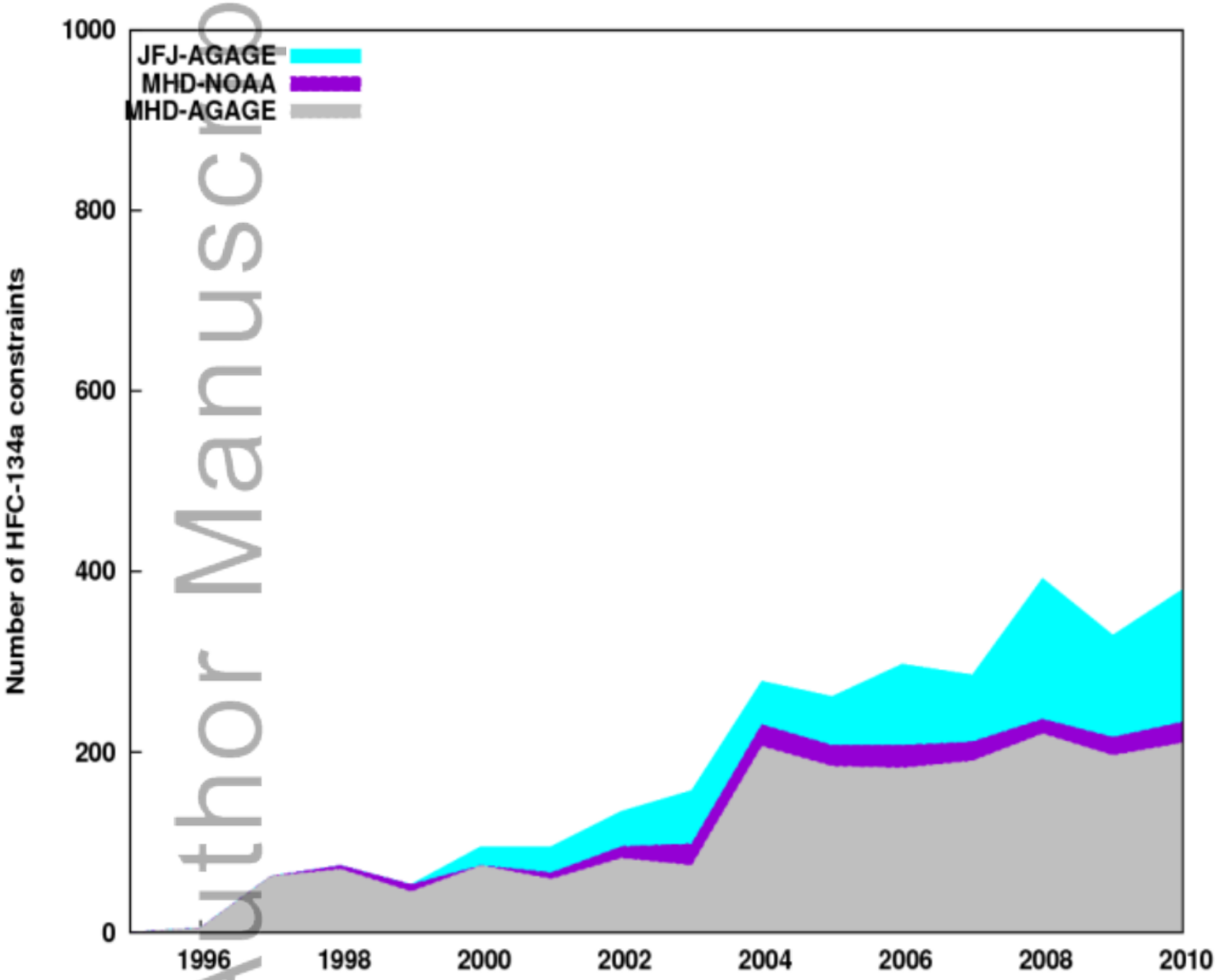

2015JD023741-f05-z-4c.png

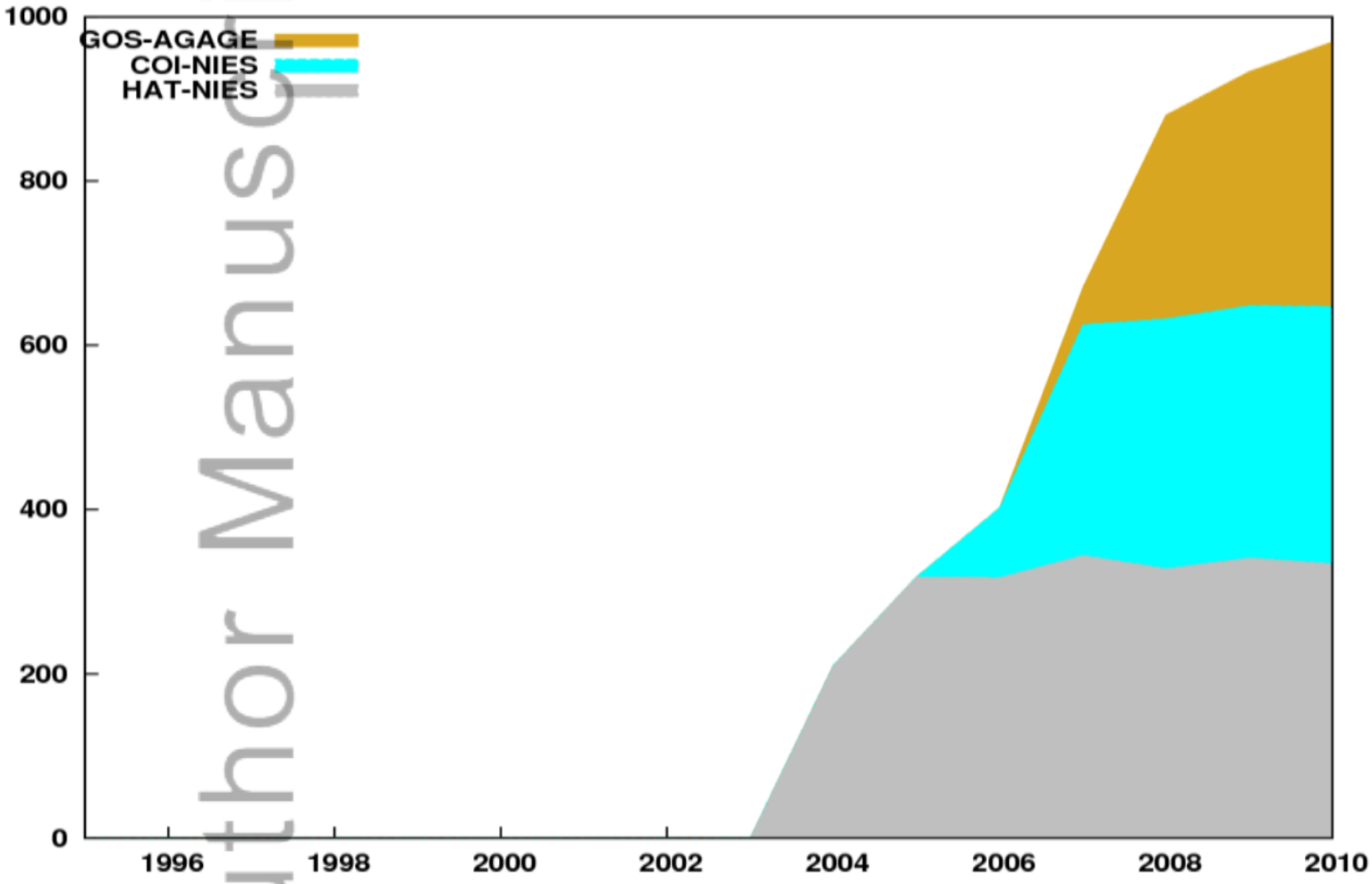

2015JD023741-f06-z-4c.png

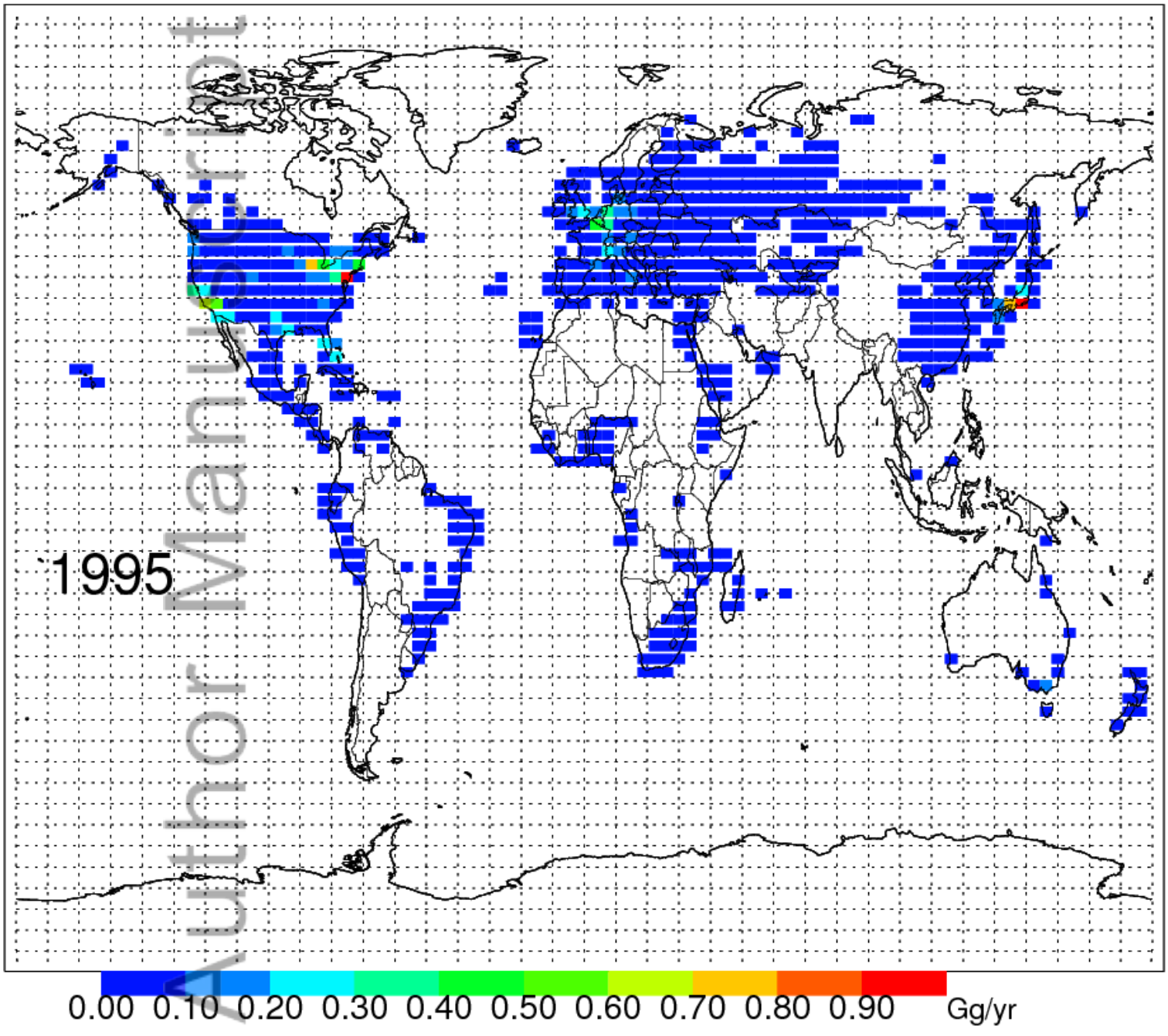

2015JD023741-f07-z-4c.png

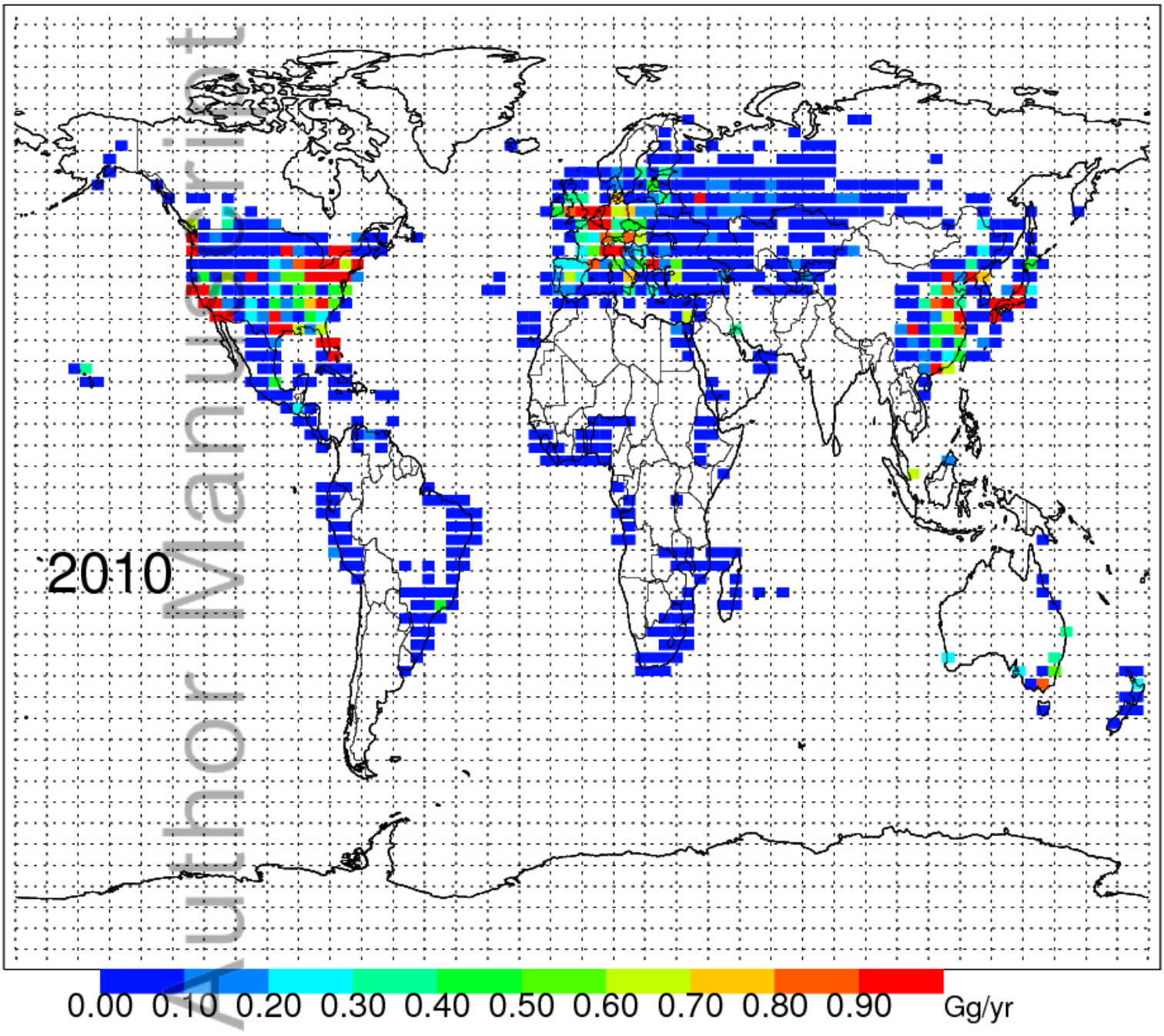

2015JD023741-f08-z-4c.png

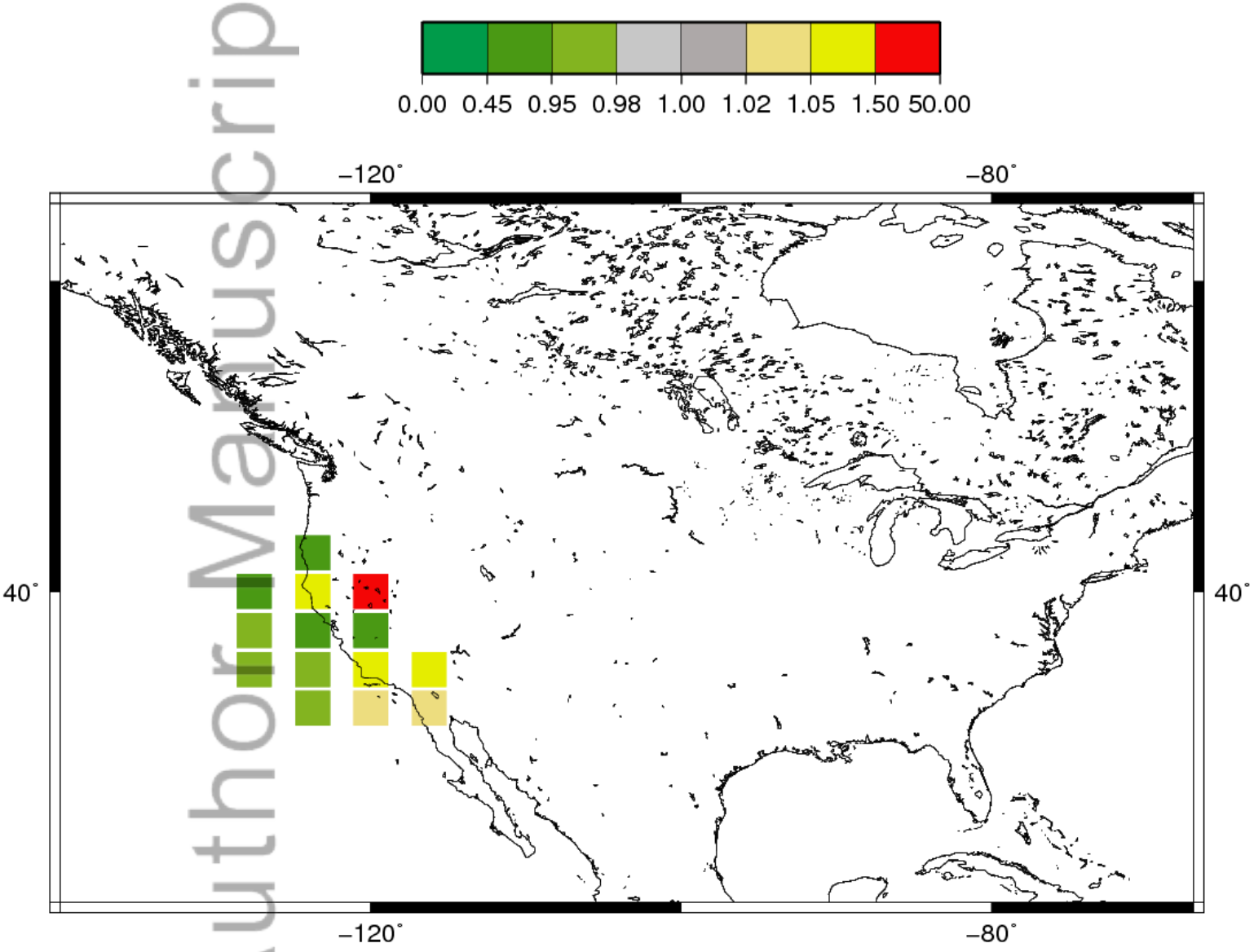

2015JD023741-f09-z-4c.png

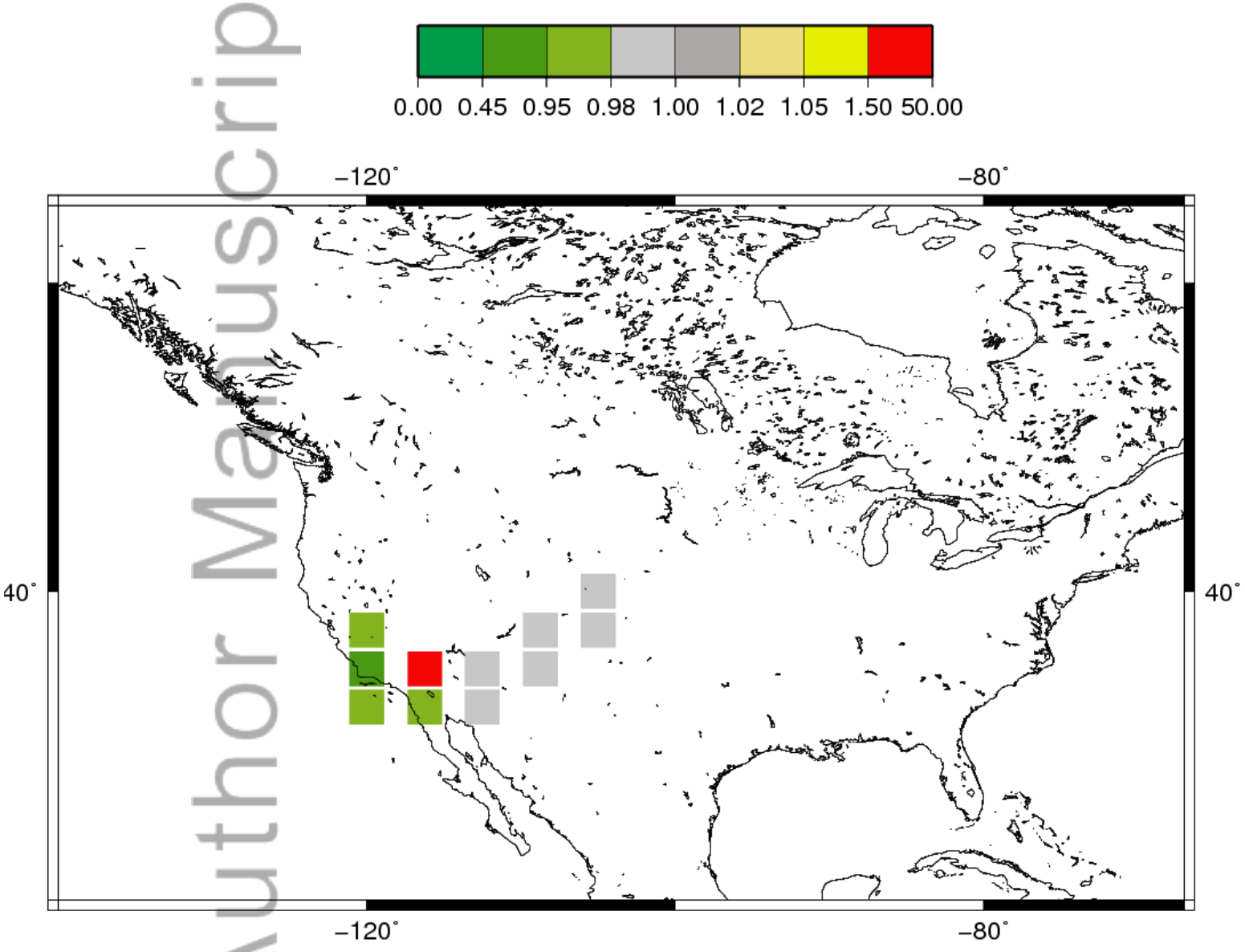

2015JD023741-f10-z-4c.png

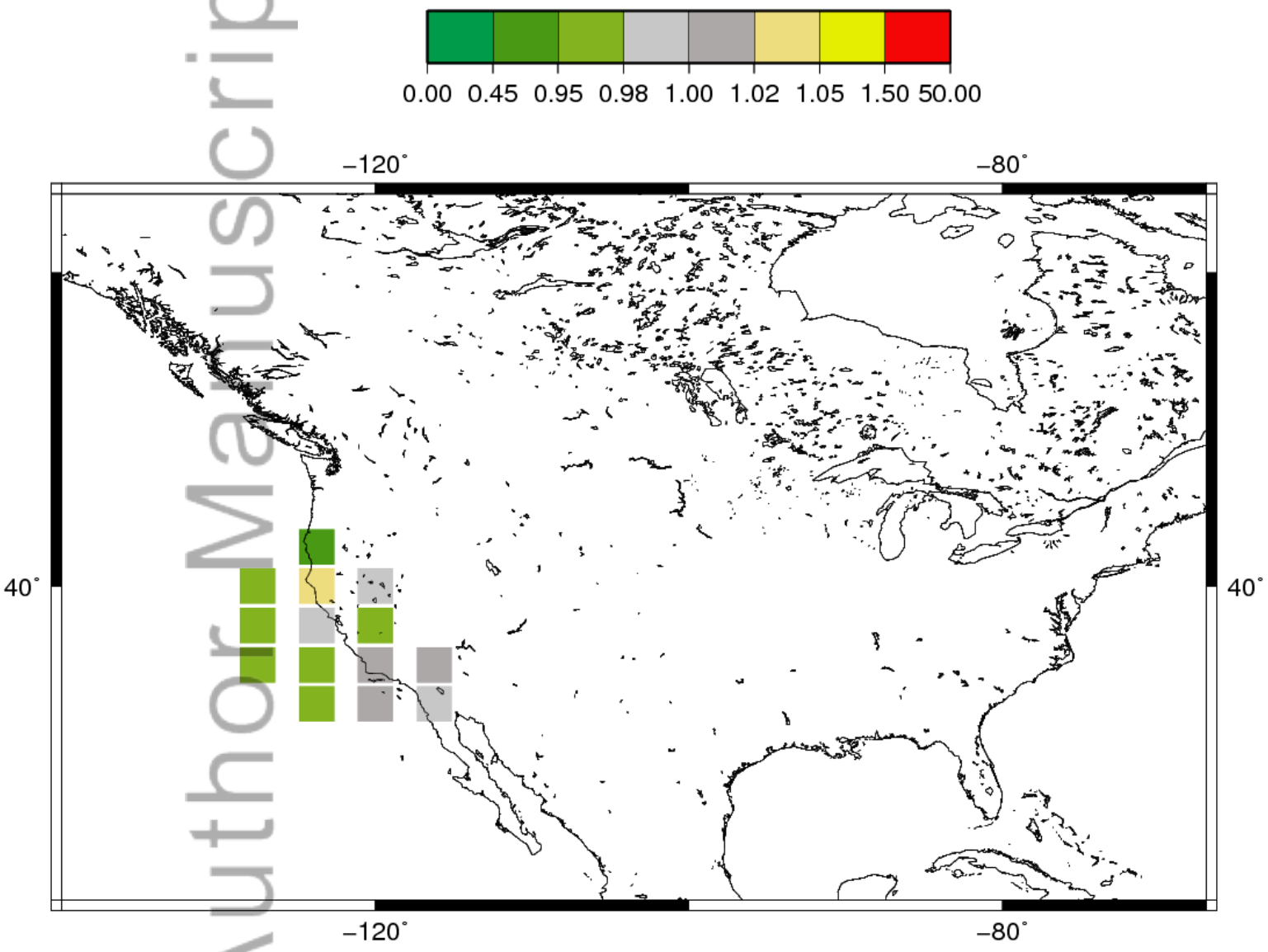

2015JD023741-f11-z-4c.png

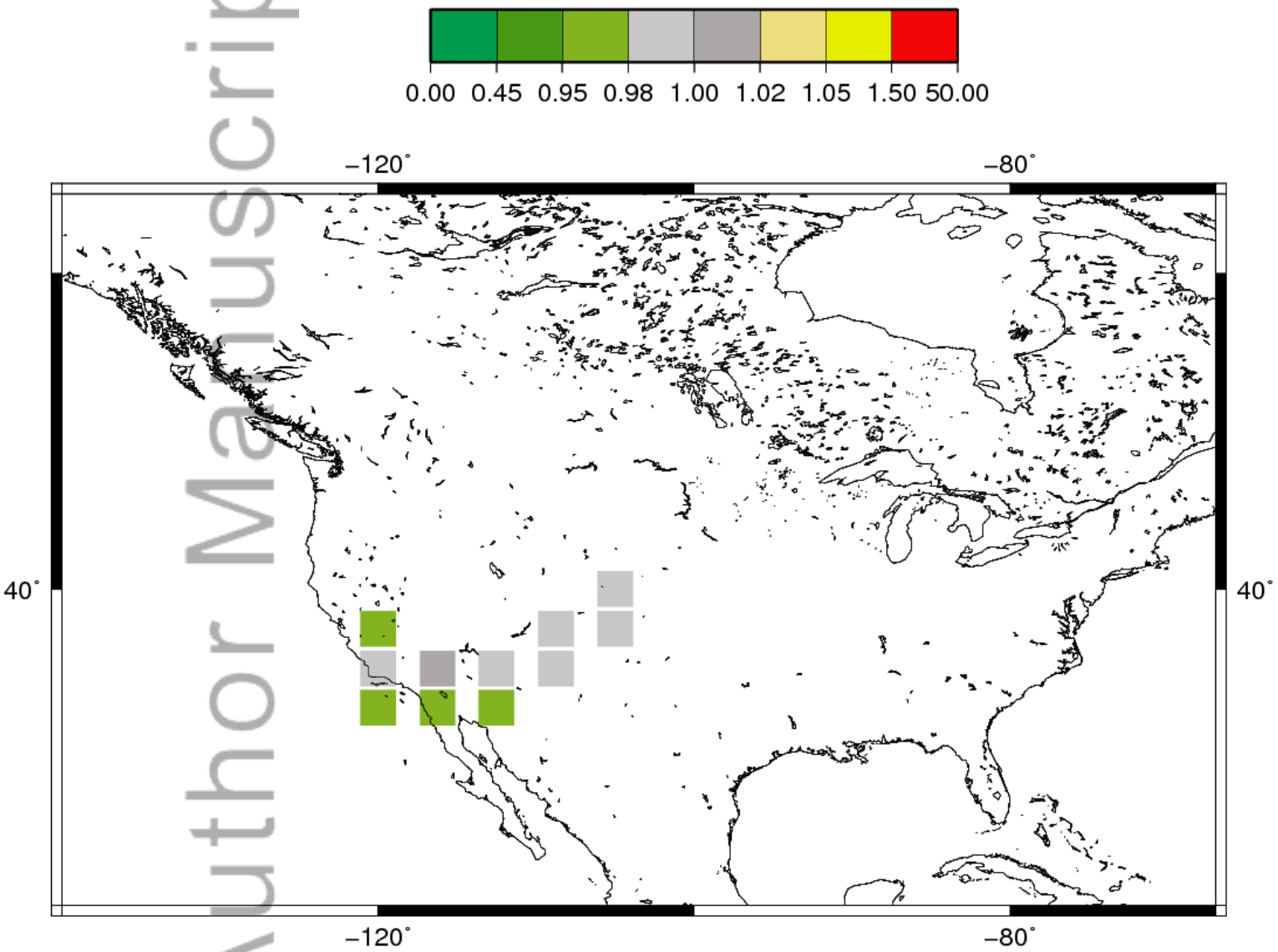

2015JD023741-f12-z-4c.png

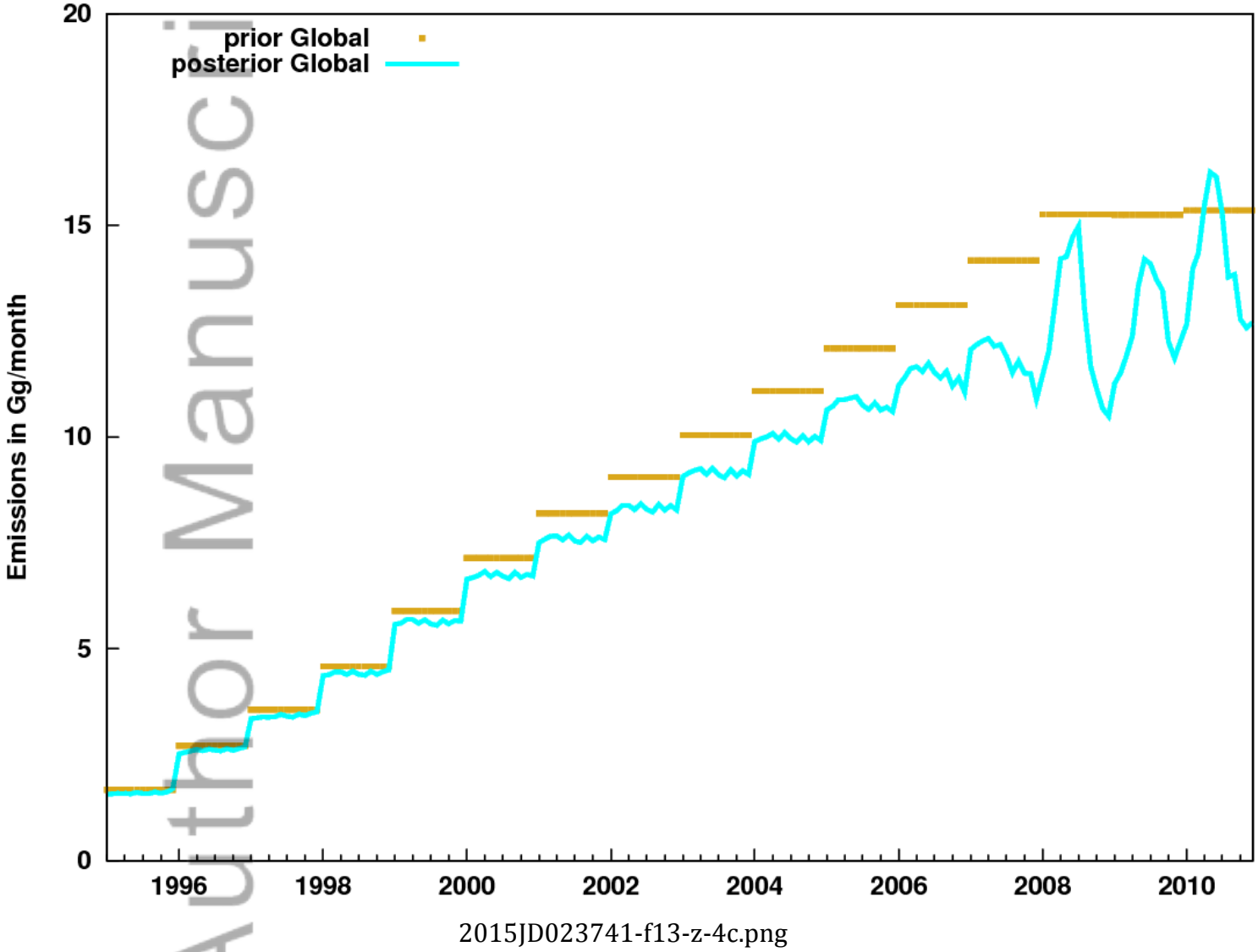

2015JD023741-f13-z-4c.png

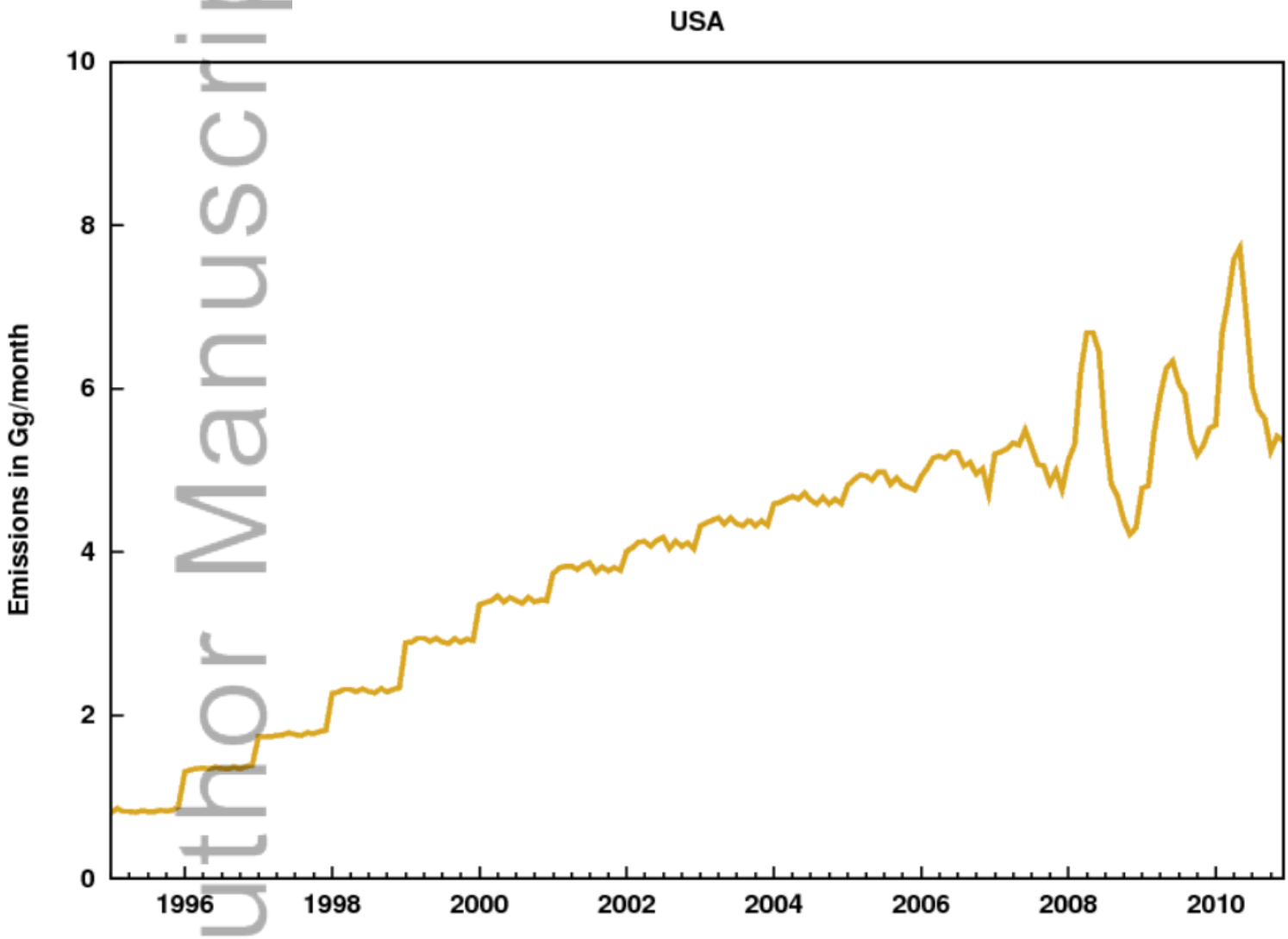

2015JD023741-f14-z-4c.png

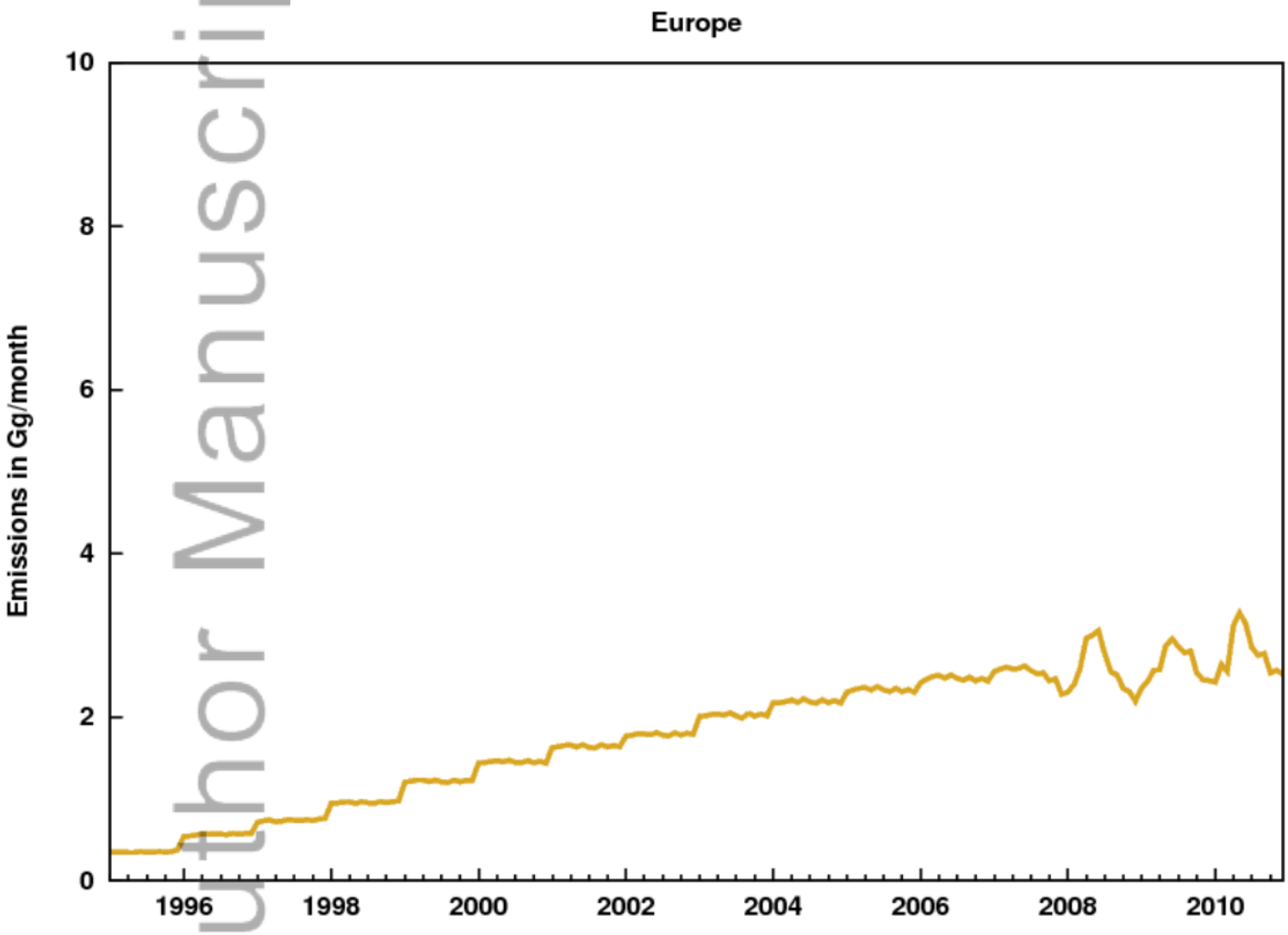

2015JD023741-f15-z-4c.png

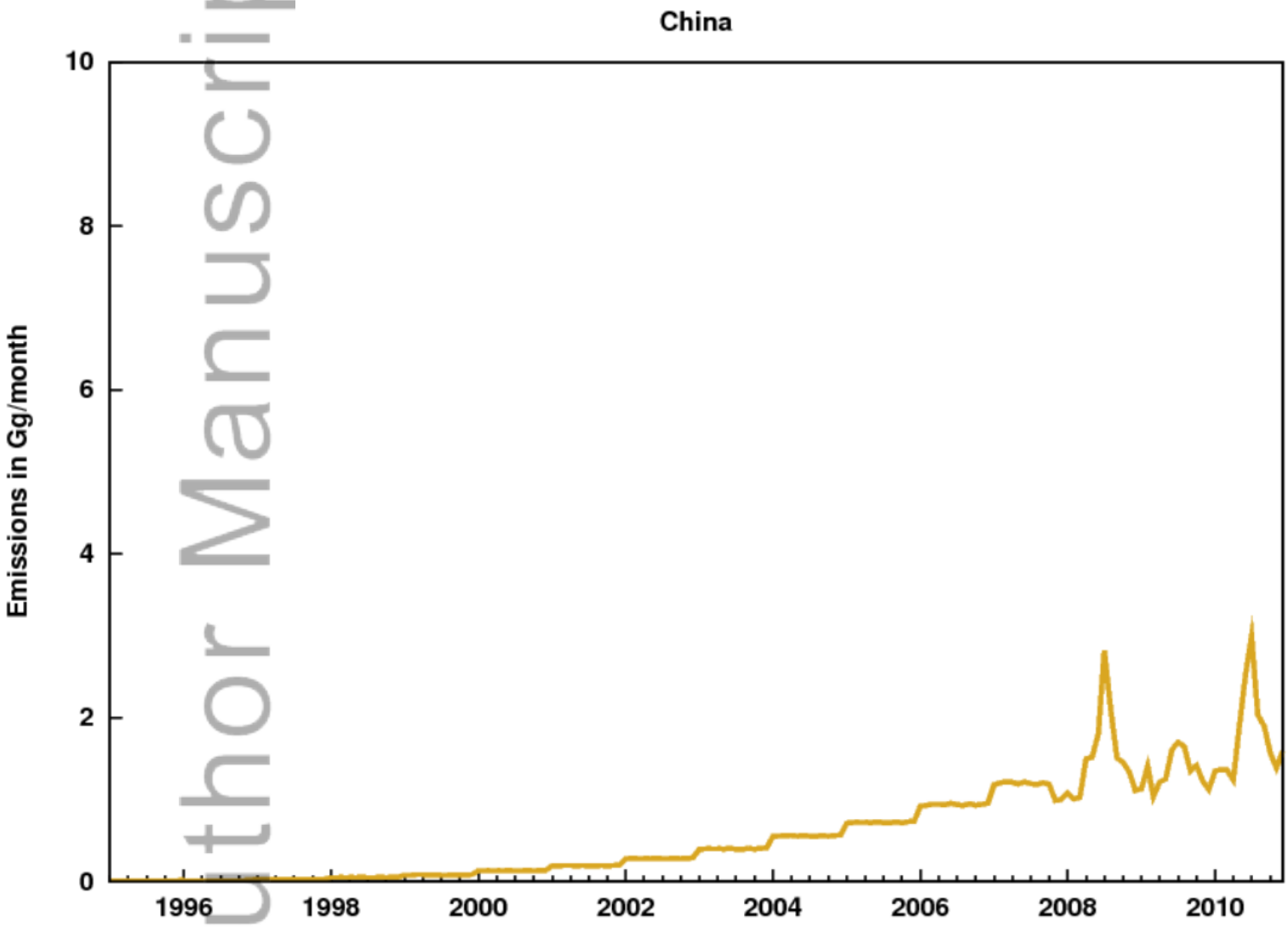

2015JD023741-f16-z-4c.png

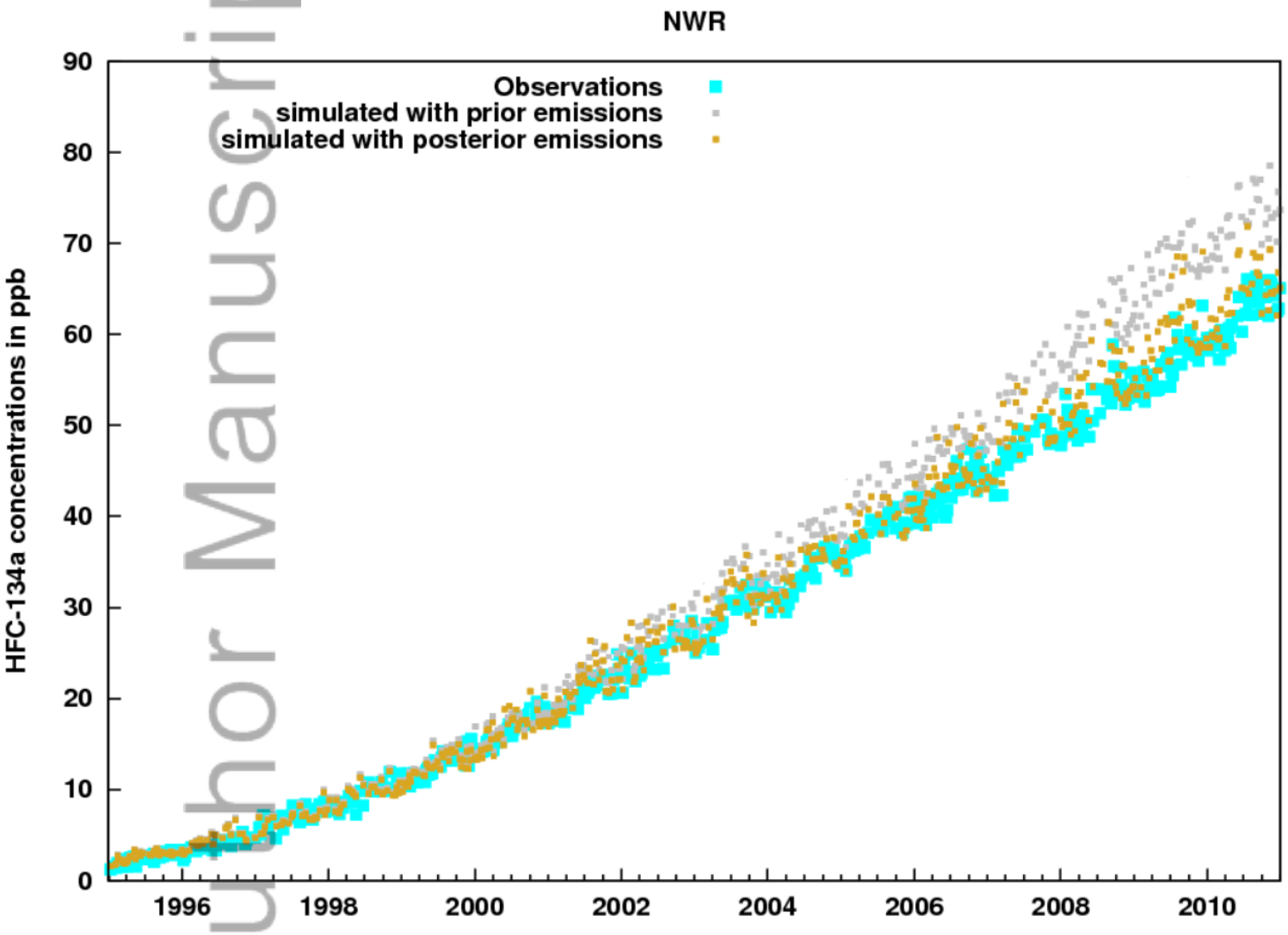

2015JD023741-f17-z-4c.png